

Contents lists available at ScienceDirect

Organic Geochemistry

journal homepage: www.elsevier.com/locate/orggeochem



Hydrogen and carbon isotope responses to salinity in greenhousecultivated mangroves



Ji Woon Park a,*, S. Nemiah Ladd a,b,c, Julian P. Sachs a

- ^a University of Washington, School of Oceanography, Seattle, WA, USA
- b Swiss Federal Institute of Aquatic Science and Technology (EAWAG), Department of Surface Waters Research and Management, Seestrasse 79, 6047 Kastanienbaum, Switzerland
- ^c Swiss Federal Institute of Technology (ETH-Zürich), Department of Earth Sciences, Sonneggstrasse 5, 8092 Zürich, Switzerland

ARTICLE INFO

Article history Received 27 July 2018 Received in revised form 26 February 2019 Accepted 5 March 2019 Available online 6 March 2019

Keywords: Mangroves Salinity Paleoclimate Hydrogen isotopes Carbon isotopes

ABSTRACT

Paired hydrogen and carbon isotope ratios (²H/¹H and ¹³C/¹²C) of mangrove lipids can be used to quantitatively reconstruct past salinity and ²H/¹H ratios of environmental water, and in some cases precipitation rate. This approach is based on the observation that net ²H- and ¹³C-fractionation increases and decreases, respectively, with the salinity of environmental water. In order to better understand the mechanisms underlying these empirical observations and ultimately improve estimates of paleoprecipitation from the paired H and C isotope approach, we analyzed the isotopic composition of fatty acids from five species of mangroves cultivated in salinity treatments of 5-30 ppt (g/kg) for 3.5 years in a greenhouse. Decreased net ¹³C-fractionation with salinity in three mangrove species was attributed to increased water use efficiency and thus a ¹³C-enriched internal CO₂ pool. Net ²H-fractionation decreased with salinity in three mangrove species, opposite to previous observations of mangroves growing along salinity gradients in lakes and estuaries. The difference between uncultivated and greenhouse-cultivated mangroves may result from variability of ²H/¹H of environmental water in natural environments. In addition, decreased net ²H-fractionation with salinity could be due to temporal variability in ²H/¹H of leaf water and timing of lipid production, and the use of stored carbohydrates in seeds. Due to the sensitivity of the salinity and ¹³C-fractionation relationship for calculating both salinity and water isotopes, optimization of mangrove lipid H and C isotopes as a paleohydrologic tracer may be best achieved through laboratory-based calibrations of the relationship between ¹³C-fractionation and salinity.

© 2019 Elsevier Ltd. All rights reserved.

1. Introduction

The tropics play an important role in global climate, as tropical convection and ocean-atmosphere interaction affect Earth's radiation budget, global water cycle and precipitation patterns (Pierrehumbert, 2000; Chiang, 2009; Wohl et al., 2012). Current climate model simulations often disagree on future precipitation projections or do not reproduce recent rainfall estimates that agree with observations, and they could be potentially improved with long-term rainfall data from paleo-precipitation proxies (Zhang et al., 2007; Flato et al., 2013; Sun et al., 2017). These proxies include tropical corals, tree rings, ice cores from alpine glaciers and marine sediment cores, but these do not provide high resolution, long-term and continuous records of precipitation in the tropics that span sub-millennial to millennial timescales (Thompson

E-mail addresses: jiwoonp@uw.edu (J.W. Park), Nemiah.Ladd@eawag.ch (S.N. Ladd), jsachs@uw.edu (J.P. Sachs).

et al., 1985, 2013; Fairbanks et al., 1997; Greer and Swart, 2006; Pfeiffer et al., 2006; Tiwari et al., 2006; Weldeab et al., 2007; Jones et al., 2009; Li et al., 2011).

A promising proxy of past tropical hydroclimate is the hydrogen isotope composition of lipids $(\delta^2 H = ((^2H/^1H_{sample})/(^2H/^1H_{VSMOW}) -$ 1) (%)) produced by photoautotrophs and preserved in organicrich lake and swamp sediments, as such sediment can provide continuous, high-resolution records on millennial timescales. δ^2H values of cyanobacterial and algal lipids are strongly correlated with $\delta^2 H$ values of source environmental water ($\delta^2 H_{water}$), both in field- and laboratory-based studies (Sauer et al., 2001; Huang et al., 2004; Englebrecht and Sachs, 2005; Zhang and Sachs, 2007; Maloney et al., 2016, 2019). Similarly, $\delta^2 H$ values of longchain n-alkanes and n-alkanoic acids produced as leaf waxes by vascular plants are also correlated with $\delta^2 H_{precipitation}$ (Sachse et al., 2004; Polissar and Freeman, 2010; Guenther et al., 2013; Tipple and Pagani, 2013). Because δ^2 H values of environmental water are strongly correlated with precipitation rate over seasonal or longer timescale in the tropics (Dansgaard, 1964; Bony et al.,

^{*} Corresponding author.

2008; Risi et al., 2008), $\delta^2 H_{water}$ values derived from measurements of $\delta^2 H_{lipid}$ of biomarkers from photosynthetic organisms can be used to calculate precipitation rate in the tropics (Smittenberg et al., 2011; Maloney et al., 2019).

However, calculating $\delta^2 H_{water}$ values (and ultimately precipitation rates) is complicated by other factors that affect $\delta^2 H_{lipid}$ values. In phytoplankton, $\delta^2 H_{lipid}$ values can be affected by temperature, salinity, light availability, biosynthetic pathway, growth rate, growth phase and source organism (Schouten et al., 2006; Zhang and Sachs, 2007; Zhang et al., 2009; Wolhowe et al., 2009; Nelson and Sachs, 2014; Heinzelmann et al., 2015a, 2015b; Sachs and Kawka, 2015; van der Meer et al., 2015; Sachs et al., 2017; Ladd et al., 2018). Similarly, $\delta^2 H_{lipid}$ values of vascular plants (including mangroves) can be affected by temperature, relative humidity, salinity, light intensity, timing of lipid synthesis and evapotranspiration (Smith and Freeman 2006; Yang et al., 2009; Feakins and Sessions 2010: Kahmen et al., 2011a, 2013: Douglas et al., 2012; Sachse et al., 2012; Tipple et al., 2013; Ladd and Sachs, 2015a, 2015b). Despite these complications, several studies have qualitatively reconstructed local precipitation in the tropics by a multi-proxy approach including $\delta^2 H_{lipid}$ values from tropical lake and marine sediments (Schefuß et al., 2005; Pahnke et al., 2007; Tierney et al., 2008; Sachs et al., 2009; Niedermeyer et al., 2010; Smittenberg et al., 2011; Konecky et al., 2013; Atwood and Sachs, 2014; Zhang et al., 2014; Richey and Sachs, 2016; Arnold

The application of leaf wax $\delta^2 H_{lipid}$ values as a precipitation proxy in coastal tropical and subtropical regions can be complicated by the strong influence of salinity on hydrogen isotope fractionation in halophilic plant leaf waxes. About a third of organic matter in tropical and subtropical coastal sediments is produced by leaf litter from mangroves, which are halophilic trees and shrubs that grow widely in the intertidal zones in the tropics and subtropics (Jennerjahn and Ittekkot, 2002; Giri et al., 2011; Alongi and Mukhopadhyay, 2015). The net fractionation factor for ²H between mangrove leaf lipids and source water (expressed as $\alpha^2 H_{lipid-water} = (\delta^2 H_{lipid} + 1000)/(\delta^2 H_{water} + 1000))$ decreases with salinity for alkanes (0.7–1.8%/ppt) and triterpenoids (0.5–0.9%/ ppt) in diverse genera of mangroves (Avicennia, Rhizophora, Bruguiera, Laguncularia) in tropical and subtropical estuaries and lakes from the western Pacific and from Florida (Ladd and Sachs, 2012, 2015a, 2015b, 2017; He et al., 2017). This suggests that if past salinity and water isotopes were to be reconstructed using $\delta^2 H_{lipid}$ values, the salinity effect can be corrected if lipids were specifically derived from mangrove trees. In contrast, using $\delta^2 H_{lipid}$ values from generic leaf wax compounds such as long-chain n-alkanes may be problematic, since these could come from mixed mangrove/nonmangrove sources and have different responses to changing precipitation rates than mangrove-sourced *n*-alkanes.

The pentacyclic triterpenoid taraxerol is particularly useful as a mangrove-specific biomarker, as it is produced in high amounts by Rhizophora spp. mangroves and is well preserved in sediments with minimal diagenetic alteration (Versteegh et al., 2004; Koch et al., 2005). $\delta^2 H_{taraxerol}$ values are influenced by both salinity and $\delta^2 H_{\text{water}}$ values, so they cannot be used on their own to estimate precipitation rate, but rather need to be paired with $\delta^2 H$ values of algal lipids that grew in the same environment with the mangroves (as in Nelson and Sachs, 2016). δ^2 H values of algal lipids are also strongly influenced by salinity, but in the opposite way to that in mangroves, as $\alpha^2 H_{lipid-water}$ in microalgae increases with salinity by 1-3%/ppt (Schouten et al., 2006; Sachse and Sachs, 2008; Sachs and Schwab, 2011; Chivall et al., 2014; M'boule et al., 2014; Nelson and Sachs, 2014; Heinzelmann et al., 2015a; Maloney et al., 2016; Sachs et al., 2016). Therefore, using the two independent linear relationships between $\alpha^2 H_{lipid-water}$ and salinity

from both mangrove and algal lipids, salinity and $\delta^2 H_{water}$ can be calculated (Ladd and Sachs, 2012; Nelson and Sachs, 2016).

A second possible approach to estimate salinity and $\delta^2 H_{water}$ is to couple $\delta^2 H$ and $\delta^{13} C$ measurements from the same mangrove leaf lipids (Ladd and Sachs, 2013). Since net $^{13}C/^{12}C$ fractionation between mangrove leaf lipids and atmospheric CO_2 ($\alpha^{13}C_{lipid-atm}$) decreases with salinity by 0.2%/pt for alkanes in *Avicennia marina* mangroves, salinity and $\delta^2 H$ of environmental water can be calculated from the linear relationships between salinity and both $\alpha^2 H$ and $\alpha^{13}C$ (Ladd and Sachs, 2013). This paired $\delta^2 H/\delta^{13}C$ approach can be improved by reducing the uncertainties in the relationship between $\alpha^{13}C_{lipid-atm}$ and salinity, as it is less well constrained than the relationship between $\alpha^2 H$ and salinity, which has been established across different lipids and mangrove taxa (Ladd and Sachs, 2012, 2015a, 2015b, 2017; He et al., 2017).

Another way to improve the accuracy of mangrove lipidderived salinity and $\delta^2 H_{\text{water}}$ estimates is to better understand the mechanisms that relate $\alpha^2 H_{lipid-water}$ and $\alpha^{13} C_{lipid-atm}$ with salinity. The relationship between $\alpha^{13} C_{lipid-atm}$ and salinity has been attributed to higher water use efficiency (WUE) with increasing salinity and increased ¹³CO₂ fixation, responses observed in both salt-tolerant and salt-sensitive plants (Farguhar et al., 1982; Brugnoli et al., 1991; Lin and Sternberg, 1992; Sobrado, 2000a; Rivelli et al., 2002; Jiang et al., 2006). The underlying mechanisms accounting for the relationship between $\alpha^2 H_{lipid-water}$ and salinity, however, are less evident. The negative α^2H -salinity relationship has been attributed to variable biosynthetic fractionation between lipids and leaf water (the direct source of hydrogen in lipids from dicots), which may be caused by differences in NADPH sources or reliance on stored carbohydrates, and variable timing of leaf or lipid production (Ladd and Sachs, 2015a, 2015b). However, in the case of B. gymnorhiza growing in marine lakes in Palau, biosynthetic fractionation did not vary with salinity, suggesting instead that the α^2 H-salinity relationship could result from a greater contribution of ²H-depleted water vapor to leaf water in a humid climate as salinity increases (Ladd and Sachs, 2017). A better understanding of these mechanisms would facilitate the use of mangrove leaf lipid δ^2 H measurements to reconstruct precipitation rates.

To improve the calibration of the relationship between mangrove leaf $\alpha^{13}C_{lipid-atm}$ and salinity by reducing uncertainty in the regression statistics, and to assess potential mechanisms causing the inverse relationship between mangrove leaf $\alpha^2H_{lipid-water}$ and salinity, five species of mangroves that employed different salt management strategies (Table 1) were cultivated in the University of Washington greenhouse for 3.5 years at six different salinity levels (5, 10, 15, 20, 25, 30 ppt (g/kg)). The δ^2H and $\delta^{13}C$ values of leaf wax fatty acids were measured along with the δ^2H values of growth water and the $\delta^{13}C$ values of bulk leaves.

2. Methods

2.1. Cultivation of mangroves in greenhouse

2.1.1. Cultivated species and greenhouse growth conditions

We cultivated five species of mangroves (Avicennia germinans, Laguncularia racemosa, Rhizophora apiculata, Rhizophora mangle, and Xylocarpus granatum), each of which relies on different mechanisms to cope with salt stress at six salinity levels (5, 10, 15, 20, 25, 30 ppt) in the Botany greenhouse at the University of Washington in Seattle. Seeds and propagules of A. germinans, L. racemosa and R. mangle were ordered from Florida Plants (Broward Co., FL, USA), while seeds of R. apiculata and X. granatum were collected during fieldwork on the islands of Pohnpei and Kosrae, Federated States of Micronesia. Seeds or propagules (40–50) of each species

Table 1Types of mangroves cultivated in the UW greenhouse and their salt management strategies (Parida and Jha, 2010; Reef and Lovelock, 2015).

Mangrove species	Exclude	Secrete	Accumulate	Salt tolerance level
Avicennia germinans	X	X	X	High
Laguncularia racemosa	X	X		Mid
Rhizophora apiculata	X		X	Mid
Rhizophora mangle	X		X	High
Xylocarpus granatum			X	Low

were germinated in water with salinity of 5 ppt during September to November 2012 and then transferred to 1 gallon pots filled with sand in the greenhouse during October to December 2012. All pots were initially supplied with 5 ppt or 10 ppt saltwater, then moved to water with higher salinity after every 4-5 days to help plants adjust to changes in salinity. A water pump pumped and drained water in the tub to a set level above the pots twice every day to simulate a mock tidal cycle. A fertilizer solution (10 mL of Peter's Plant Food solid with 1 L water) was added to all plants weekly. In the greenhouse, temperature ranged between 15.5 °C and 23 °C, relative humidity ranged between 25% and 90%, and light levels between October and April were supplemented by P.L. Light system (600 W). While temperature and relative humidity are expected to be higher in humid tropical climates where these mangrove species grow naturally, field conditions could not be more closely simulated due to other experiments that were conducted in the greenhouse at the same time. Because about half of R. apiculata were not growing well, additional R. apiculata from Kosrae were added in September 2013, and R. apiculata in poor health were removed between November 2013 and January 2014.

2.1.2. Tub water salinity and $\delta^2 H$ maintenance

Saltwater was produced by adding Instant Ocean Sea Salt to tap water. Salinity was monitored daily with a conductivity probe (Amprobe WT-60), and 2–3 L of tap water was added whenever evaporation caused salinity to increase by 0.5 ppt.

In January 2013 it was observed that the tub water isotopes had become enriched relative to the starting tap water. To counteract evaporative enrichment after this point, 10 L of water in each tub was replaced with 10 L of freshly prepared salt water $(\delta^2 H = -70\%e)$ every week to maintain relatively constant $\delta^2 - H_{water} = \sim -50\%e$ over time across all salinity tubs, and tub water samples for $\delta^2 H$ measurements were collected weekly before and after water replacement.

2.1.3. Harvest

In order to monitor isotopic variability in leaves over time, one leaf from each R. mangle tree was collected and placed into a plastic bag (WhirlPak, Hach, CO, USA) in July 2014 and stored in a freezer at $-20\,^{\circ}\mathrm{C}$ until further analysis. In March 2016 all trees were completely harvested. For each plant, plant mass above the sand surface, wet root mass and dry root mass was recorded. Leaves were cut off from stem, placed in plastic bags and stored at $-20\,^{\circ}\mathrm{C}$. Roots were cleaned with water, dried in the oven overnight and stored at $-20\,^{\circ}\mathrm{C}$.

Development of mangrove seedlings in the greenhouse may have been constrained by temperature and pot size. The temperature range in the greenhouse was lower than that of typical mangrove habitats (20–30 °C), which may have subjected trees to cold stress (Duke, 2006). Limited pot size can also constrain root growth, resulting in reduced photosynthesis and plant biomass (Arp, 1991; Kasai et al., 2012; Poorter et al., 2012). In addition, placing plants inside pots itself can significantly affect root morphology, reducing capability of the roots to take up water efficiently (NeSmith and Duval, 1998).

2.2. Extraction and purification of lipids from leaves

For each species, from the group of trees grown in the same salinity treatment, two or three trees with healthy-looking leaves were selected. Strips along the midrib from 2-4 leaves of the same tree were freeze-dried and ground together to average out isotopic heterogeneity among leaves or across the base and tip of a single leaf. Total lipid extracts were extracted by Accelerated Solvent Extraction (ASE) following methods previously described by Ladd and Sachs (2015a). The resulting total lipid extract from all species except R. mangle was saponified to separate fatty acids and neutral compounds (including alkanes and sterols). Each dry sample was heated at 70 °C for 3 h after adding 3 mL of 1 N KOH/MeOH and 2 mL HPLC-grade H₂O and cooled to room temperature. Hexane (2 mL) was added to the saponified samples and vortexed, and the organic phase (containing neutral compounds) was transferred to new vials. After 4-5 hexane rinses, 15-20 drops of 4 N HCl was added to the saponified samples to decrease the pH below 2. Then, 2 mL of hexane was added 4-5 times to the acidic saponified samples and vortexed, and the organic phase (containing protonated fatty acids) was transferred to new vials. For R. mangle, in order to separate alkanes and triterpenoids from other types of neutral compounds, the lipid extracts were purified using column chromatography methods previously described by Ladd and Sachs (2015a).

A 2% aliquot of fatty acids and alcohols from all species was silylated by adding 20 µL pyridine and 20 µL BSTFA at 60 °C for 1 h. Lipid composition was identified by gas chromatography-mass spectrometry (GC-MS) with an Agilent (Santa Clara, CA, USA) 6890N gas chromatograph with an Agilent 5975 quadrupole mass selective detector and an Agilent DB-5 column $(60 \text{ m} \times 0.25 \text{ mm} \times 0.25 \text{ } \mu\text{m})$ with helium as the carrier gas (1.1 mL/min flow). The GC was heated initially to 100 °C for 2.1 min, then at 5 °C/min to 320 °C for 23.9 min. Compounds were identified based on retention times and comparisons with published mass spectra.

Half of the remaining 98% of the acid fraction was methylated with the methylating agent prepared by adding 5 mL of acetyl chloride to 50 mL of anhydrous methanol chilled in an ice bath. Dry hexane (1 mL) and 2 mL of methylating agent was added to each sample, vortex-mixed and heated in an oven at 60 °C for 24 h. After cooling samples to room temperature, 2 mL of HPLCgrade H₂O and 2 mL of hexane were added, vortex-mixed and separated three times. Half of the remaining 98% of the sterol fraction from R. mangle leaves was acetylated by adding 20 µL pyridine and 20 μ L acetic anhydride with known δ^2 H composition at 70 °C for 30 mins. 5α -cholestane was added as a quantification standard to 25-75% aliquots of methylated samples. The samples were quantified on an Agilent 6890 N gas chromatograph (GC) with flame ionization detector (GC-FID) and an Agilent VF-17 ms column $(60 \text{ m} \times 0.25 \text{ mm} \times 0.25 \text{ } \mu\text{m})$ with helium (1.4 mL/min) as the carrier gas. The GC was heated initially to 100 °C for 2.1 min, then at 5 °C/min to 320 °C where it was held for 23.9 min.

The saponification, isolation, and derivatization of fatty acids as described does not result in detectable isotope fractionation

(Zhang and Sachs, 2007; Smittenberg et al., 2011; Sachs and Kawka, 2015; Maloney et al., 2016; Sachs et al., 2017, 2018).

2.3. Lipid $\delta^2 H$ and $\delta^{13} C$ analysis

Fatty acid samples from all five mangrove species were diluted with toluene to a concentration of \sim 150 ng/ μ L (for δ^2 H analyses) or \sim 40 ng/ μ L (for δ^{13} C analyses) prior to measurement by gas chromatography-isotope ratio mass spectrometry (GC-IRMS) at the University of Washington on equipment described previously (Ladd and Sachs, 2015a). For fatty acid analysis, an Agilent DB-5 ms column ($60 \text{ m} \times 0.25 \text{ mm} \times 0.25 \text{ }\mu\text{m}$) was used, with helium as the carrier gas (1.5 mL/min flow). The GC was initially heated to 120 °C, then at 20 °C/min to 180 °C, then at 3 °C/min to 325 °C and held for 16 min. Alkanes and triterpenols from R. mangle were diluted to the same concentrations, and analyzed using an Agilent VF-17 ms $(60 \text{ m} \times 0.25 \text{ mm} \times 0.25 \text{ } \mu\text{m})$, also with helium as the carrier gas (1.1 mL/min flow). The GC was initially heated to 120 °C, then at 20 °C/min to 260 °C, then at 1 °C/min to 300 °C, and then at 20 °C/min to 325 °C and held for 18.5 min. Each sample was injected three times for each isotope measurement.

Performance of the instrument was evaluated by running a mix of external standards (C_{21} , C_{23} , C_{28} , C_{32} , C_{34} , C_{38} n-alkanes) after every 4 or 5 samples and co-injecting a mix of internal standards (C_{26} , C_{32} , C_{38} n-alkanes) with each sample. All n-alkane isotopic reference standards and their $\delta^2 H$ and $\delta^{13} C$ values were provided by A. Schimmelmann, University of Indiana. The average standard deviations of the external standards were 2.8% for $\delta^2 H$ analyses and 0.26% for $\delta^{13} C$ analyses.

Raw $\delta^2 H$ and $\delta^{13} C$ values from the instrument were corrected using Thermo ISODAT software V. 2.5 as described previously (Ladd and Sachs, 2015a). Fatty acid $\delta^2 H$ and $\delta^{13} C$ were corrected for methylation using a phthalic acid standard with known $\delta^2 H = -95.5 \pm 2.2\%$ and $\delta^{13} C = -27.21 \pm 0.02\%$ (data from A. Schimmelmann) that was methylated and measured in the same way as the fatty acid samples. The H_3^+ factor was determined at the start of each sequence, using pulses of a reference gas of varying heights, and was 1.66 ± 0.07 during November 2016 and March 2017 when *A. germinans, L. racemosa, R. apiculata* and *R. mangle* samples were analyzed, and 2.04 when *X. granatum* samples were analyzed in February 2018.

 $\delta^2 H$ values of triterpenols in leaves from 2014 and 2016 in each salinity treatment were averaged to calculate $\alpha^2 H_{2016\text{-}2014} = (\delta^2 H_{2016} + 1000)/(\delta^2 H_{2014} + 1000)$ in each salinity at each time, and fractionation factors between *R. mangle* lipids harvested in 2014 and 2016 were calculated with the equation ϵ_{2016} $_{-2014}$ = $(\alpha^2 H_{2016\text{-}2014} - 1) \times 1000$ (%) (Supplementary Table S3).

2.4. Source water δ^2 H analysis

 $\delta^2 H$ values of tub water samples ($\delta^2 H_{water}$) collected between July 2014 and March 2016 were measured by Cavity Ring Down Spectroscopy following the methods described by Ladd and Sachs (2015a), and the average precision of the final three injections was 0.33% for $\delta^2 H$.

Fractionation factors of 2H between lipids and environmental water ($\alpha^2H_{lipid-water}$) at harvest were calculated using the last two measured δ^2H_{water} values (from February and March 2016) in order to represent as closely as possible the isotopic composition of water used to synthesize the leaf lipids, since fatty acids in plant leaf waxes are recycled every few days (Gao et al., 2012) and the δ^2H_{water} values increased over time (Supplementary Fig. S1).

2.5. Bulk leaf $\delta^{13}C$ analysis

Leaves (1–3) from the same trees selected for lipid $\delta^{13}C$ analysis were oven-dried at 60 °C for 24 h, then left at room temperature for 24 h to prevent over-drying, and ground to a fine powder. About 4 mg of each leaf powder was enclosed in tin capsules and sent to the UC Davis Stable Isotope Facility for bulk leaf $\delta^{13}C$ analysis on a PDZ Europa ANCA-GSL elemental analyzer connected to a PDZ Europa 20–20 isotope ratio mass spectrometer (Sercon Ltd., Cheshire, UK). The samples were combusted in an oxidation reactor filled with chromium oxide and silver copper oxide at 1000 °C with helium flow, producing N_2 , CO_2 , water and oxides. To remove water and oxides these products went through a reduced copper reactor and a magnesium perchlorate water trap. CO_2 and N_2 were separated on a Carbosieve GC column (65 °C, 65 mL/min) before entering the IRMS for isotope analysis.

2.6. Leaf water model

 $\delta^2 H$ values of leaf water $(\delta^2 H_{lw})$ were calculated using a Péclet-modified Craig Gordon model from Kahmen et al. (2011b), as described previously by Ladd and Sachs (2015b, 2017). The modeled $\delta^2 H_{lw}$ values were used to compare the effect of salinity on $\delta^2 H_{lw}$ in the greenhouse and to evaluate if the influence of salinity on $\delta^2 H_{lw}$ can account for differences in $\delta^2 H_{lipid}$ across a salinity gradient. Initially, a sensitivity test was performed with the leaf water model by calculating the range of $\delta^2 H_{lw}$ values from end-member values of one variable at a time while holding the other variables constant. The range of temperature and relative humidity is as described in Section 2.1.1, and the range of $\delta^2 H_{atmospheric\ vapor}$ was determined from measurements with an isotopic water vapor analyzer (Los Gatos Research, San Jose, CA) during 2013 January.

The range of stomatal conductance (g_s) (rate of water vapor loss, $mol/m^2/s$) encompasses published observations from *A. germinans, L. racemosa and R. mangle* leaves (Lin and Sternberg, 1992; Sobrado, 2000a, 2000b; Krauss and Allen, 2003; Biber 2006). The range of effective path length (L, mm) was derived from published values in several species of mangroves (Ellsworth et al., 2013; Liang et al., 2018). The range of $\delta^2 H$ values of xylem water ($\delta^2 H_{xw}$) was calculated using published α_{xw-sw} values (Ladd and Sachs, 2015b) and measured $\delta^2 H_{water}$ values, and accounts for the fractionation due to discrimination against $^2 H$ at roots during water uptake that has been observed in mangroves (Lin and Sternberg, 1993). As $\delta^2 H_{water}$ values in the greenhouse were relatively stable (Supplementary Fig. S1), and α_{xw-sw} decreases at high salinity (Lin and Sternberg, 1993; Ladd and Sachs, 2015b), $\delta^2 H_{xw}$ values are expected to be $^2 H$ -depleted at high salinity in our case.

Among the variables included in the model, stomatal conductance, $\delta^2 H_{xylem\ water}$ and effective path length were identified to vary directly with salinity. We assessed the variation in $\delta^2 H_{lw}$ values from changes in these three factors across the 25 ppt salinity range, but did not account for species-specific differences in the factors, as the results of our sensitivity test suggested that the effects of species-specific variations in these variables are not as significant as effects from other variables common across species (Table 2, Supplementary Table S1). In our final calculations, gs of R. mangle from Lin and Sternberg (1992) (0.35 mol/m²/s at 5 ppt and 0.15 $mol/m^2/s$ at 30 ppt) was used. L at 5 and 30 ppt were estimated using the inverse relationship between L and transpiration rate (Song et al., 2013), where the transpiration rate at each salinity was calculated from the g_s values above. $\delta^2 H_{lw}$ values at 5 ppt and 30 ppt were calculated with the leaf water model using endmembers of these three variables while keeping other variables constant (Table 3).

In addition, to assess the diurnal isotopic variability of leaf water, different "daytime" and "nighttime" temperature, relative

Table 2Test of leaf water model sensitivity. As each variable in the first column changed within the range shown in the second column, other variables were held constant.

	Input	$\delta^2 H_{lw}$ (‰)	Range of $\delta^2 H_{lw}$
Temperature (°C)	16 ± 3 to 23 ± 3	-31 ± 3 to -38 ± 3	7‰
Relative humidity (%)	25 ± 5 to 90 ± 5	$-28 \pm 11 \text{ to}$ -39 ± 4	11‰
$\delta^2 H_{atmospheric\ vapor}$ (‰)	-110 ± 5 to -125 ± 5	-32 ± 3 to -44 ± 3	12‰
Stomatal conductance (g _s ; mol/m ² s)	0.1 ± 0.05 to 0.4 ± 0.05	-41 ± 3 to -38 ± 3	3‰
Effective path length (L; mm)	$150 \pm 50 \text{ to}$ 300 ± 50	-48 ± 3 to -44 ± 3	4‰
$\delta^2 H_{xylem \ water} (\%)$	-42 ± 5 to -48 ± 5	-35 ± 3 to -37 ± 3	2‰

humidity and atmospheric vapor δ^2H values (Table 4) were used to calculate daytime and nighttime δ^2H_{lw} values. A daytime temperature of 21 °C and a nighttime temperature of 17 °C were employed for this calculation. Relative humidity was estimated using water vapor content and saturated vapor pressure calculated from temperature.

An estimate of uncertainty for modeled $\delta^2 H_{lw}$ values was derived from a Monte Carlo approach with 1000 iterations that included the uncertainties for all model variables.

2.7. Statistical analysis

Simple ordinary least square regression was used to calculate the correlations between $\delta^2 H,~\delta^{13} C$ or $\alpha^2 H_{lipid-water}$ and salinity. To account for different magnitude of standard errors in the triplicate $\delta^2 H$ and $\delta^{13} C$ measurements, a 1000 iteration Monte Carlo analysis was used to normally distribute errors from $\delta^2 H$ and $\delta^{13} C$ measurements and reassign the random uncertainties to each data point to calculate slopes and intercepts.

3. Results

3.1. Relationship between salinity and $\delta^{13}C_{\text{fatty acid}}$

Out of five species, three (L. racemosa, R. apiculata and X. granatum) had significant (p < 0.05) positive correlations between salinity and $\delta^{13}C_{\text{fatty acid}}$ (R² = 0.51 for *L. racemosa n*-C₁₈, 0.45 for *R.* apiculata n-C₁₆, 0.69 for R. apiculata n-C₁₈, 0.35 for X. granatum n-C₁₆ and 0.36 for X. granatum n-C₁₈) (Fig. 1; Table 5). Slopes of the relationship between salinity and $\delta^{13}C_{\text{fatty acid}}$ calculated from ordinary least square regression were similar in L. racemosa and R. apiculata $(0.123 \pm 0.008 \text{ for } R. \text{ apiculata } n\text{-}C_{16}, \ 0.207 \pm 0.009 \text{ for } R.$ apiculata n- C_{18} , 0.207 \pm 0.009 for L. racemosa n- C_{18}), while slopes from X. granatum were about half as steep $(0.086 \pm 0.006 \text{ for } n$ C_{16} , 0.095 ± 0.009 for n- C_{18}). Fatty acids from X. granatum $(-38.1 \pm 1.4\%)$ were more depleted than fatty acids from L. racemosa and R. apiculata (each $-34.1 \pm 2.3\%$ and $-33.3 \pm 1.9\%$) (Supplementary Table S2). In contrast, the other two species (A. germinans and R. mangle) did not have significant relationships between salinity and $\delta^{13}C_{fatty acid}$.

Table 3 Inputs used for leaf water model to calculate $\delta^2 H_{leaf\ water}$ at 5 and 30 ppt salinity levels.

Salinity (ppt)	g _s (mol/m ² /s)	L (mm)	$\delta^2 H_{xylem \ water} (\%)$	$\delta^2 H_{leaf\ water}$ (‰)
5	0.35	120	-42	-36.1 ± 2.6
30	0.15	280	-48	-38.9 ± 3.0

3.2. Relationship between salinity and $\delta^{13}C_{bulk\ leaf}$

A significant positive correlation (p < 0.05) between salinity and $\delta^{13}C_{\text{bulk leaf}}$ was observed in *L. racemosa* (R² = 0.90), *R. apiculata* (R² = 0.74) and *X. granatum* (R² = 0.56) (Fig. 2; Table 6). Slopes of the relationship calculated from ordinary least square regression were of a similar order to the slopes of salinity vs $\delta^{13}C_{\text{fatty acid}}$ (0.164 ± 0.020 for *L. racemosa*, 0.220 ± 0.034 for *R. apiculata* and 0.101 ± 0.021 for *X. granatum*). *R. mangle* showed a significant negative correlation between salinity and $\delta^{13}C_{\text{bulk leaf}}$ (p = 0.032, R² = 0.26, m = -0.070 ± 0.030), while *A. germinans* did not show a significant correlation (p = 0.555).

3.3. Relationship between salinity and $\delta^2 H_{fatty\ acid}$

Three of the five species (R. apiculata, R. mangle and X. granatum) displayed significant (p < 0.05) correlations between salinity and $\delta^2 H_{\rm fatty~acid}$ (Fig. 3; Table 5). In all three, $\delta^2 H_{\rm fatty~acid}$ values were positively correlated with salinity (R^2 = 0.48 for R. apiculata n- C_{16} , 0.31 for R. apiculata n- C_{18} , 0.39 for R. mangle n- C_{16} and 0.22 for X. granatum n- C_{18}). The slopes of the relationships between salinity and $\delta^2 H_{\rm fatty~acid}$ calculated from ordinary least square regression were greater in R. apiculata (1.253 \pm 0.113 and 1.179 \pm 0.113 each for n- C_{16} and n- C_{18} fatty acids) than in either R. mangle (0.474 \pm 0.142 for n- C_{16} fatty acid) or X. granatum (0.529 \pm 0.060 for n- C_{18} fatty acid).

 $\alpha^2 H_{lipid\text{-water}}$ values were also positively correlated with salinity for *R. apiculata* and *R. mangle* (R^2 = 0.48 for *R. apiculata* $n\text{-}C_{16}$, 0.31 for *R. apiculata* $n\text{-}C_{18}$, and 0.36 for *R. mangle* $n\text{-}C_{16}$), but the correlation was not significant in *X. granatum* (p = 0.105) (Fig. 4; Table 5). Lipids from the other two species (*A. germinans* and *L. racemosa*) did not display significant relationships between either $\delta^2 H_{fatty\ acid}$ and salinity or $\alpha_2 H_{lipid\text{-water}}$ and salinity.

3.4. Leaf water model results

Results of the sensitivity test show that modeled $\delta^2 H_{lw}$ values are more sensitive to changes in $\delta^2 H_{vapor}$ values, relative humidity and temperature, than they are to changes in stomatal conductance and effective path length (Table 2).

As salinity increased from 5 ppt to 30 ppt, stomatal conductance was estimated to decrease from 0.35 mol/m²/s to 0.15 mol/m²/s (Lin and Sternberg, 1992), $\delta^2 H_{xw}$ values were estimated to be $^2 H$ -depleted by 7.6‰, and path length was estimated to increase from 120 mm to 280 mm. These variables ultimately resulted in modeled $\delta^2 H_{lw}$ values that are depleted by 2.7‰ at 30 ppt relative to 5 ppt (Table 3). $\delta^2 H_{lw}$ values were more depleted under daytime conditions $(-42.2 \pm 3.4\%)$ than under nighttime conditions $(-25.9 \pm 2.8\%)$.

3.5. $\delta^2 H_{triterpenoids}$ in R. mangle leaves harvested in 2014 and 2016

 $\delta^2 H$ values of three triterpenoids (taraxerol, β -amyrin and lupeol) were more $^2 H$ -depleted in 2016 than in 2014 in 15 of 18 *R. mangle* treatments (Fig. 5; Supplementary Table S2). There were no statistically significant relationships (at p < 0.05) between salinity and $\delta^2 H_{triterpenoids}$ of *R. mangle* harvested in either year, or

 $\begin{tabular}{ll} \textbf{Table 4} \\ \textbf{Inputs used for leaf water model to calculate } $\delta^2 H_{leaf \ water}$ in daytime and nighttime. \end{tabular}$

	Temperature	Water vapor content	Relative humidity	$\delta^2 H_{atmospheric\ vapor}$
Day	21 ± 2 °C	15000 ppm	0.97 ± 0.10	-125 ± 5‰
Night	17 ± 2 °C	12000 ppm	1.00 ± 0.10	$-110 \pm 5\%$

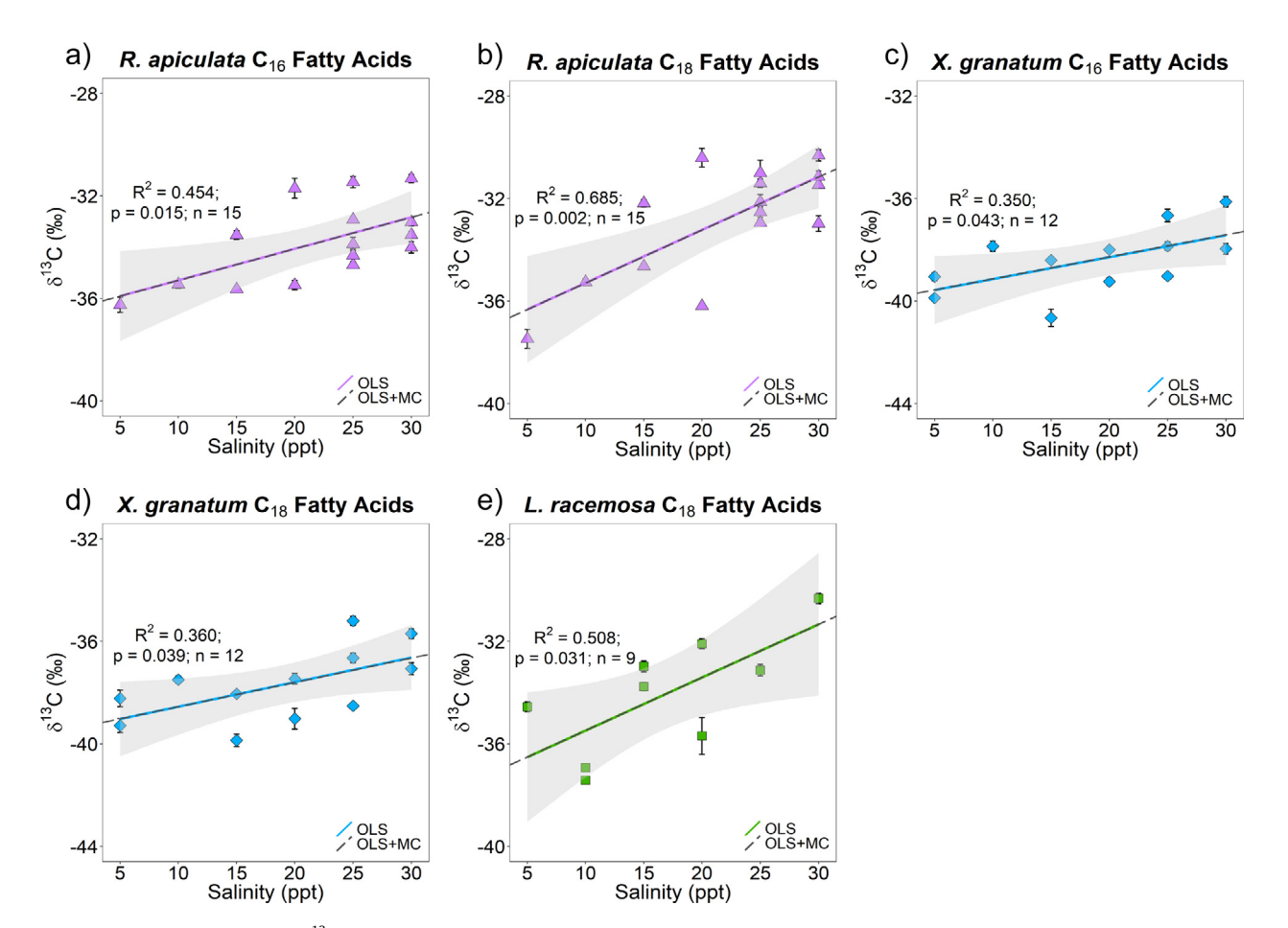


Fig. 1. Relationships between salinity and δ^{13} C_{fatty acid} in mangrove leaf lipids. All linear regression equations and statistics are listed in Table 5. Panels only show species and compounds that display significant relationship (p < 0.05). All panels include the regression lines (colored solid lines, labeled "OLS"), regression lines from Monte Carlo analysis (gray dashed lines, labeled "OLS + MC") and 95% confidence intervals (gray shaded areas). Error bars that are not displayed are smaller than the plot marker size.

between salinity and ϵ_{2016} – $_{2014}$ for any of the three triterpenoids (Supplementary Table S1).

4. Discussion

4.1. Relationships between salinity and $\delta^{13}C_{\text{fatty acid}}$ of cultivated mangroves

4.1.1. Effect of water use efficiency on $\delta^{13}C_{fatty\ acid}$ and $\delta^{13}C_{bulk\ leaf}$ The significant positive correlation between $\delta^{13}C_{bulk\ leaf}$ values and salinity of cultivated *L. racemosa*, *R. apiculata* and *X. granatum* observed in this study (Table 6) is consistent with past studies (Farquhar et al., 1982; Sobrado, 2000a; Ladd and Sachs, 2013). This has been attributed to increased WUE at high salinity, which results in limited exchange of CO_2 between the atmosphere and the intercellular air space under high salinity treatments and more

Generally, the observed correlation between $\delta^{13}C_{bulk}$ leaf and salinity (R² range 0.56–0.90) is stronger than that between $\delta^{13}C_{fatty}$

incorporation of ¹³C into leaf lipids from a ¹³C-enriched internal

CO₂ pool (Farguhar et al., 1982, 1989).

 $_{
m acid}$ and salinity (R 2 range 0.35–0.69) (Tables 5 and 6). The correlation between $_{
m N}^{13}C_{
m bulk}$ $_{
m leaf}$ and salinity in greenhouse-cultivated trees is also much higher than that in uncultivated trees (Ladd and Sachs, 2013). This strong relationship may have resulted from the nitrogen fertilizer we supplied to the greenhouse-cultivated mangroves. Martin et al. (2010) observed that N-fertilized A. marina have higher WUE than trees without fertilizer, possibly because the additional nitrogen was allocated to Rubisco to keep up with high carbon assimilation rates. Since the greenhouse-cultivated trees were supplied with nitrogen fertilizers throughout their growth, it may be possible that greenhouse-cultivated trees had higher WUE and reduced intercellular CO $_2$ concentration relative to uncultivated trees, resulting in a relatively strong positive trend between salinity and $_{
m N}^{13}C_{
m bulk\ leaf}$ values.

There were no significant correlations between salinity and δ^{13} - $C_{\text{fatty acid}}$ or $\delta^{13}C_{\text{bulk leaf}}$ in *A. germinans* and *R. mangle*. These two species are highly salt-tolerant, and maintain high WUE across wide ranges of salinity (Reef and Lovelock, 2015). If these species can lower water potential by efficiently secreting through salt glands (*A. germinans*) or accumulating solutes in cytoplasm (*A. germinans* and *R. mangle*) (Table 1), they may rely relatively less on

Table 5Results of linear regression analysis between salinity and $\delta^2 H_{\text{fatty acid}}$ or $\delta^{13} C_{\text{fatty acid}}$ in all mangrove species and two fatty acid compounds.

Isotopes	Species	N	Compound	Slope	Intercept	MC slope	MC intercept	R ²	р
$\delta^2 H_{\text{fatty acid}}$	A. germinans	10	n-C ₁₆	-0.38 ± 0.24	-94.52 ± 5.04	-0.38 ± 0.04	-94.49 ± 0.82	0.237	0.153
O Tifatty acid	71. germinans	10	n-C ₁₈	-0.35 ± 0.24 -0.11 ± 0.35	-64.26 ± 7.28	-0.11 ± 0.12	-64.22 ± 3.42	0.012	0.764
	L. racemosa	9	n-C ₁₆	0.03 ± 0.21	-160.41 ± 3.75	0.04 ± 0.06	-160.43 ± 0.78	0.005	0.858
	2. racemosa	J	n-C ₁₈	0.51 ± 0.40	-148.10 ± 7.23	0.50 ± 0.09	-148.03 ± 1.73	0.189	0.242
	R. apiculata	15	n-C ₁₆	1.25 ± 0.36	-115.81 ± 8.41	1.25 ± 0.11	-115.82 ± 2.77	0.479	0.004
	·· F · · · · · · · · · · · · · · · · · · ·		n-C ₁₈	1.18 ± 0.49	-100.13 ± 11.34	1.18 ± 0.11	-100.07 ± 2.58	0.310	0.031
	R. mangle	15	n-C ₁₆	0.47 ± 0.17	-88.89 ± 3.31	0.47 ± 0.14	-88.97 ± 3.41	0.388	0.017
	X. granatum	13	n-C ₁₆	0.15 ± 0.23	-93.51 ± 4.59	0.15 ± 0.04	-93.51 ± 0.84	0.012	0.529
	Ü		n-C ₁₈	0.53 ± 0.24	-96.29 ± 4.87	0.53 ± 0.06	-96.31 ± 1.40	0.221	0.051
$\delta^{13}C_{fatty\ acid}$	A. germinans	10	n-C ₁₆	-0.01 ± 0.08	-33.97 ± 1.71	-0.01 ± 0.03	-33.98 ± 0.71	0.001	0.934
,			n-C ₁₈	0.02 ± 0.08	-32.92 ± 1.67	0.02 ± 0.03	-32.90 ± 0.61	0.009	0.797
	L. racemosa	9	n-C ₁₆	0.18 ± 0.12	-39.17 ± 2.17	0.18 ± 0.02	-39.13 ± 0.93	0.244	0.176
			n-C ₁₈	0.21 ± 0.08	-37.55 ± 1.41	0.21 ± 0.01	-37.54 ± 0.14	0.508	0.031
	R. apiculata	15	n-C ₁₆	0.12 ± 0.04	-36.53 ± 1.02	0.12 ± 0.01	-36.53 ± 0.19	0.454	0.015
	_		n-C ₁₈	0.21 ± 0.05	-37.36 ± 1.21	0.21 ± 0.01	-37.37 ± 0.21	0.685	0.002
	R. mangle	15	n-C ₁₆	-0.03 ± 0.02	-39.31 ± 0.46	-0.03 ± 0.01	-39.33 ± 0.18	0.092	0.292
	X. granatum	12	n-C ₁₆	0.09 ± 0.04	-40.00 ± 0.76	0.09 ± 0.01	-40.00 ± 0.12	0.350	0.043
			n-C ₁₈	0.10 ± 0.04	-39.51 ± 0.83	0.10 ± 0.01	-39.50 ± 0.19	0.360	0.039
$\alpha^2 H_{lipid-sw}$	A. germinans	10	n-C ₁₆	-0.00044 ± 0.00028	0.950 ± 0.006	-0.00049 ± 0.00108	0.951 ± 0.027	0.236	0.154
•			n-C ₁₈	-0.00011 ± 0.00035	0.935 ± 0.007	-0.00010 ± 0.00103	0.935 ± 0.026	0.012	0.764
	L. racemosa	9	n-C ₁₆	0.00000 ± 0.00025	0.881 ± 0.005	0.00001 ± 0.00105	0.881 ± 0.024	0.000	0.992
			n-C ₁₈	0.00051 ± 0.00040	0.851 ± 0.007	0.00051 ± 0.00107	0.851 ± 0.024	0.189	0.242
	R. apiculata	15	n-C ₁₆	0.0013 ± 0.0004	0.928 ± 0.008	0.0012 ± 0.0014	0.928 ± 0.035	0.484	0.004
			n-C ₁₈	0.0012 ± 0.0005	0.899 ± 0.011	0.0011 ± 0.0014	0.901 ± 0.034	0.310	0.031
	R. mangle	15	n-C ₁₆	0.0005 ± 0.0002	0.956 ± 0.004	0.0004 ± 0.0018	0.957 ± 0.043	0.356	0.024
	X. granatum	13	n-C ₁₆	0.0000- ± 0.0002	0.953 ± 0.005	0.0000 ± 0.0001	0.955 ± 0.024	0.001	0.910
			n-C ₁₈	0.0004 ± 0.0002	0.906 ± 0.005	0.0003 ± 0.0009	0.908 ± 0.022	0.221	0.105

Columns "MC slope" and "MC intercept" refer to results obtained from Monte Carlo approach. Relationships that are significant at the p < 0.05 level are indicated in bold letters.

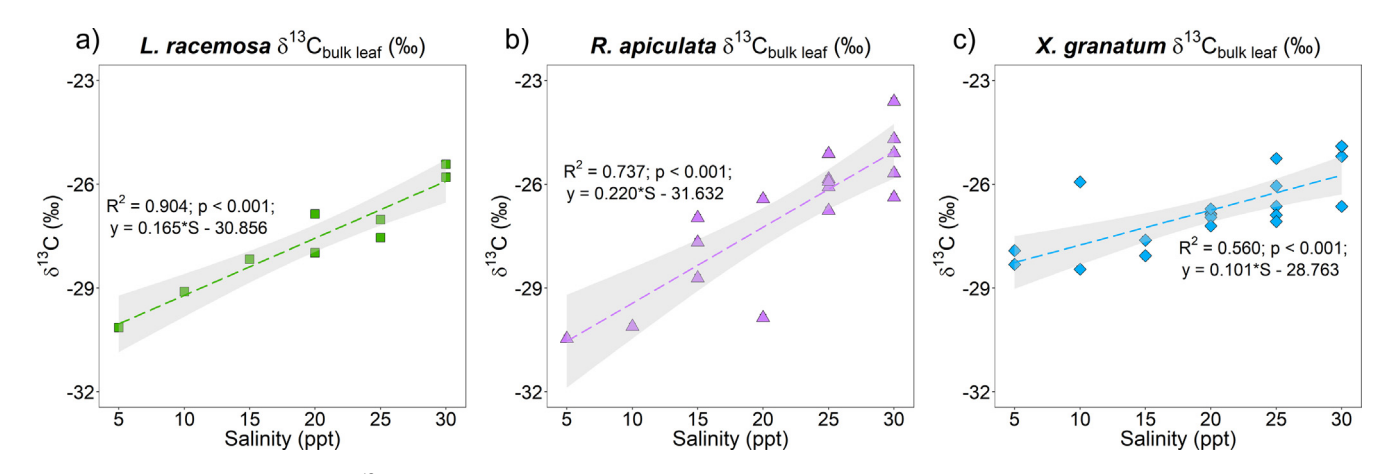


Fig. 2. Relationships between salinity and $\delta^{13}C_{\text{bulk leaf}}$ in mangrove leaf lipids. All linear regression equations and stastics are listed in Table 6. Panels only show species that display significant positive relationship (p < 0.05). All panels show the regression lines (colored dashed lines) and 95% confidence intervals (gray shaded areas). Error bars that are not displayed are smaller than the plot marker size.

 $\label{eq:continuous} \textbf{Table 6}$ Results of linear regressions between salinity and $\delta^{13}C_{bulk\ leaf}$ in all five mangrove species.

Isotopes	Species	N	Slope	Intercept	R^2	p
$\delta^{13}C_{bulk\ leaf}$	A. germinans	17	-0.030 ± 0.050	-28.445 ± 1.024	0.024	0.555
	L. racemosa	9	0.164 ± 0.020	-30.858 ± 0.416	0.904	0.000
	R. apiculata	17	0.220 ± 0.034	-31.632 ± 0.767	0.737	0.000
	R. mangle	18	-0.070 ± 0.030	-25.845 ± 0.567	0.257	0.032
	X. granatum	20	0.101 ± 0.021	-28.763 ± 0.448	0.560	0.000

Relationships that are significant at the p < 0.05 level are indicated in bold letters.

stomatal opening and closure to minimize water loss. However, while mangrove species with salt glands (*Aegiceras corniculatum*, *Aegialitis annulata*, *A. marina*) have been observed to lack relationships between salinity and $\delta^{13}C_{\text{bulk leaf}}$ (Guy et al., 1988), some of the same species (*A. corniculatum* and *A. marina*) have also been

observed to have lower stomatal conductance and carbon assimilation rate with increasing salinity, despite high solute concentrations in their leaves (Ball and Farquhar, 1983). Therefore, while the lack of correlation between salinity and $\delta^{13}C_{\text{fatty}}$ acid or $\delta^{13}C_{\text{bulk}}$ leaf values suggests that A. germinans and R. mangle may

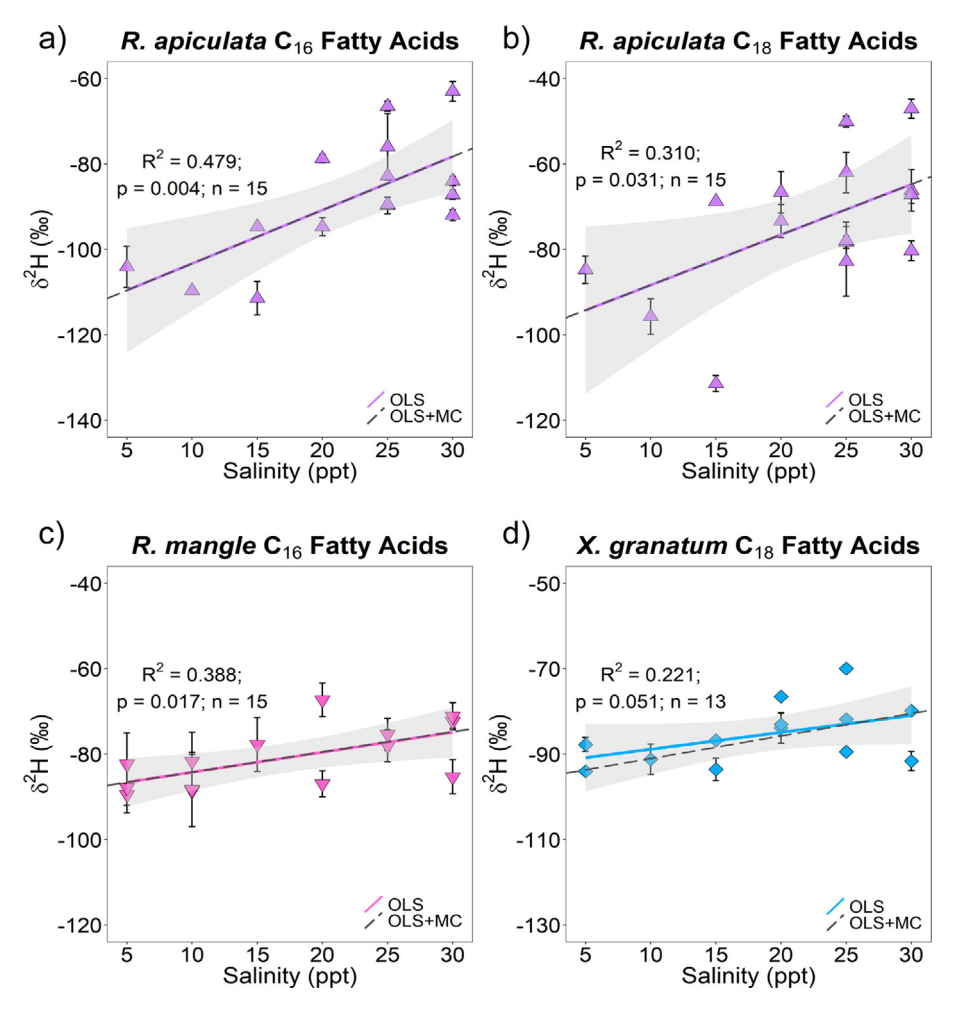


Fig. 3. Relationships between salinity and δ^2 H_{fatty acid} in mangrove leaf lipids. All regression equations and statistics are listed in Table 5. Panels only show species and compounds that display significant relationship (p < 0.05). All panels include the regression lines (colored solid lines), regression lines from Monte Carlo analysis (gray dashed lines) and 95% confidence intervals (gray shaded areas). Error bars that are not displayed are smaller than the plot marker size.

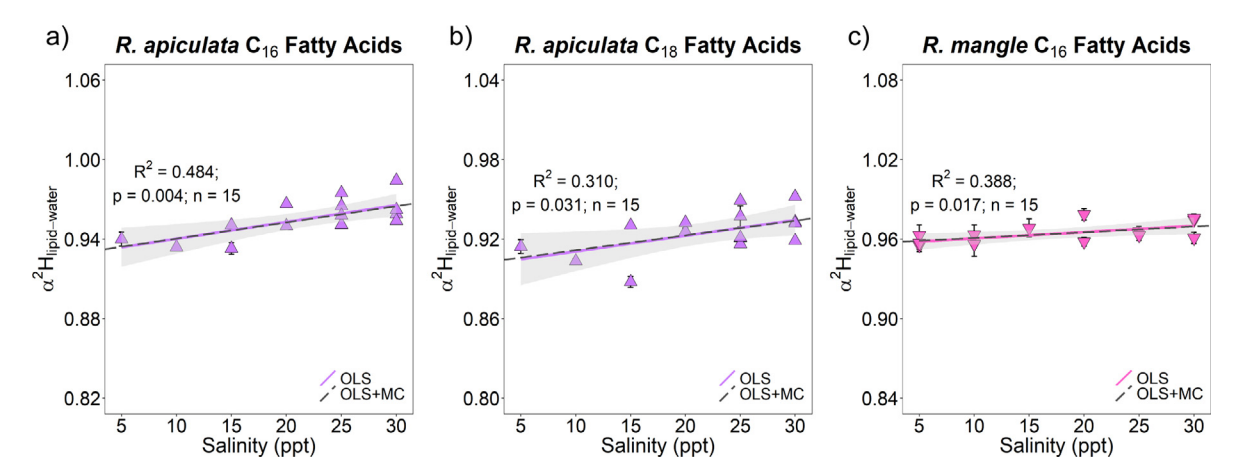


Fig. 4. Relationships between salinity and $\alpha^2 H_{lipid-water}$ in mangrove leaf lipids. All regression equations and statistics are listed in Table 5. Panels only show species and compounds that display significant relationship (p < 0.05). All panels include the regression line (colored solid lines), regression line from Monte Carlo analysis (gray dashed lines) and 95% confidence intervals (gray shaded areas). Error bars in each panel represent propagated uncertainties from $\delta^2 H_{lipid}$ and $\delta^2 H_{water}$ measurements, and those that are not displayed are smaller than the plot marker size.

adjust their water potentials by excluding excess salt rather than limiting water loss through the stomata, additional studies are required to establish the significance of these salt exclusion strategies in maintaining high WUE.

4.1.2. Plant growth correlated with salinity and $\delta^{13}C_{fatty\ acid}$

Dry root mass and wet plant mass are good measures of halophilic plant growth. With increasing salinity, halophilic plants increase root mass to obtain water, reinforce cell-wall lignification

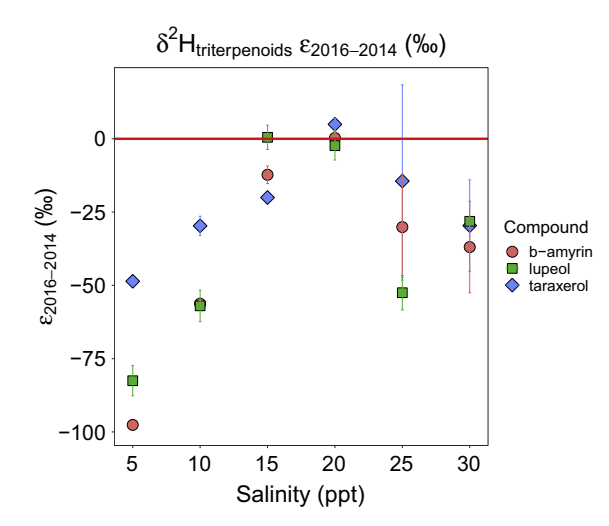


Fig. 5. Relationships between salinity and $\delta^2 H_{\text{triterpenoids}}$ in *R. mangle* leaf lipids. Y axis values show the fractionation between lipids harvested in 2016 and 2014 ($\epsilon_{2016-2014}$). Red solid line ($\delta^2 H = 0\%$) is drawn for reference. Error bars that are not displayed are smaller than the plot marker size. (For interpretation of the references to colour in this figure legend, the reader is referred to the web version of this article.)

to limit salt absorption (Cheng et al., 2012; Vovides et al., 2014), and decrease stomatal conductance and carbon assimilation rates (Ball and Farguhar, 1983); therefore, plants under high salt stress are expected to have higher dry root mass and lower wet plant mass. In our study, L. racemosa and X. granatum displayed a decrease in total wet mass as salinity increased (Supplementary Fig. S2), implying that growth was suppressed at high salinity. This observation is consistent with the suggestion above that these species decrease their stomatal conductance to increase WUE, and further supports the explanation that WUE is primarily responsible for the positive correlation between salinity and $\delta^{13}C_{bulk\ leaf}$. Meanwhile, dry root mass of all five species decreased or did not change significantly with increasing salinity (Supplementary Fig. S3), which may suggest that factors other than salinity, such as lower temperature and relative humidity or limited pot size, may have had larger influences on the growth of greenhouse-cultivated mangroves. However, as environmental factors in the greenhouse other than salinity were equally imposed on all plants, carbon isotope fractionation observed in fatty acids and bulk lipids in greenhouse-cultivated mangroves is likely controlled by increased WUE in response to salinity.

Nevertheless, given that the positive correlations between $\delta^{13}C_{lipid}$ and salinity in three different species of cultivated mangroves (*L. racemosa, R. apiculata* and *X. granatum*) were similar to that in the field (Ladd and Sachs, 2013), incorporating a larger set of greenhouse-cultivated and uncultivated samples may help to decrease uncertainty in the relationship between $\alpha^{13}C$ and salinity for some mangrove species.

4.2. Relationships between salinity and $\delta^2 H_{\text{fatty acid}}$ of greenhouse mangroves

4.2.1. Differing trends among cultivated and uncultivated mangroves Field studies have documented negative correlations between salinity and $\alpha^2 H_{\text{lipid-water}}$ of various lipids (including $n\text{-}C_{29}$ and $n\text{-}C_{31}$ alkanes, taraxerol, stigmasterol, and sitosterol) from different mangrove species in diverse settings, including lakes and estuaries in Australia, Palau, Micronesia, and Florida (Ladd and Sachs, 2012, 2015a, 2015b, 2017; He et al., 2017). These published results differ

from the positive correlations observed in greenhouse-cultivated R. *apiculata* and R. *mangle* in this study (Fig. 4; Table 5). The discrepancy may be due to differences in environmental parameters between the field and the greenhouse, such as $\delta^2 H_{\text{water}}$, or to different responses of individual lipid compounds to salinity (Ladd and Sachs, 2012, 2015a, 2015b, 2017; He et al., 2017).

A major difference between field and greenhouse settings is that there are alternate fresh or less-saline water sources that may be utilized by trees in the field. Several studies have proposed that mangroves opportunistically take up fresh or less-saline water through their roots during precipitation events (Lambs et al., 2008; Wei et al., 2013; Santini et al., 2015) or from groundwater (Ewe et al., 2007; Sternberg and Swart, 1987), or through their leaves when wetted by rain or dew (Reef and Lovelock, 2015; Steppe et al., 2018). Hydrogen and oxygen isotope mixing models have been used to determine quantitative contributions of different water sources, such as soil water, groundwater, and rainwater. Studies estimated that scrub A. marina use 37-93% rainwater, R. stylosa use 21-41% groundwater and 14-20% dew and L. racemosa use 24% groundwater and 9% dew (Wei et al., 2013; Lovelock et al., 2017). Since freshwater is more depleted in ²H than seawater, field trees under high salt stress may have been more dependent on opportunistic freshwater uptake than trees under low salt stress, resulting in the production of lipids that are more ²H-depleted relative to the surface water from which net $\alpha^2 H_{lipid-water}$ values are calculated (Ladd and Sachs, 2017). Unlike in the field, where rain, dew, and low-salinity water sources may be at least sporadically available to mangroves, in the greenhouse, $\delta^2 H_{water}$ was held relatively constant across the 25 ppt salinity range. Supplementary Fig. S1 shows that while growth water became slightly more ²Henriched over ~ 1.5 years, differences in $\delta^2 H_{water}$ across salinities were about 8‰, which is small relative to the observed differences between δ^2H of freshwater and saline water in the field (about 30%) (Ladd and Sachs, 2015b). Therefore, the lack of strong positive correlation between $\alpha^2 H_{lipid\text{-water}}$ and salinity in greenhousecultivated trees may be due to the fact that, unlike trees in the field, they had no access to water with different δ^2 H values than that provided in the growth tubs. In addition, while the field studies (Ladd and Sachs, 2012, 2015b, 2017) found that the correlation coefficient between salinity and $\alpha^2 H_{lipid-water}$ was higher than that between salinity and $\delta^2 H_{lipid}$, our results show that the strength of the two correlations are about the same, or even lower in the case of X. granatum. The strong correlations of $\delta^2 H_{water}$ values with salinity in the field (through the mixing of freshwater with a low δ^2 H value and seawater with a high δ^2 H value) are additive to the tendency of mangroves to fractionate ²H from ¹H to a greater extent at high salinity, and stable $\delta^2 H_{water}$ values across salinity treatments in the greenhouse may therefore have resulted in weaker observed relationships between $\alpha^2 H_{lipid-water}$ and salinity.

Other differences between natural environments and greenhouse settings such as temperature may have contributed to different trends between uncultivated and greenhouse-cultivated mangrove-derived lipids and salinity. It is unclear what effect temperature would have on hydrogen isotope fractionation in mangroves, as this has not been studied directly. However, in growth chamber experiments with other vascular plants, temperature did not affect hydrogen isotope fractionation during lipid biosynthesis (Zhou et al., 2011). Additionally, since all mangroves in our study were exposed to the same temperature conditions regardless of salinity treatment, any possible effect of temperature on α^2H would have affected plants in all salinity treatments equally. However, it may be possible that cold temperature imposed significant cold stress on all greenhouse plants so that the temperature effect outweighed changes in isotopic fractionation due to differences in salinity, resulting in a different relationship between salinity and $\delta^2 H_{lipid}$ from that of uncultivated trees.

It is also possible that parameters not controlled in the greenhouse experiments, such as nutrient availability or water temperature, co-varied with salinity in the field sites and were responsible for the observed relationships between salinity and $\alpha^2 H_{lipid-water}$. However, considering that the same relationship between salinity and $\alpha^2 H_{lipid-water}$ has been observed across diverse settings in the tropics and subtropics (Ladd and Sachs, 2012, 2015a, 2015b, 2017; He et al., 2017), this seems unlikely.

It is noteworthy that all $\delta^2 H_{lipid}$ values we report here from greenhouse-cultivated mangroves are from $n-C_{16}$ and $n-C_{18}$ fatty acids, while the field studies focused on n-alkanes and triterpenoids. This study focused on fatty acids as they have shorter residence time in leaves than other lipid compounds and would reflect conditions at time of sampling more closely (Sachse et al., 2009; Kahmen et al., 2011a; Gao et al., 2012). However, the significant correlation between salinity and R. mangle $\delta^2 H_{fatty\ acid}$ (Fig. 3) and lack of any correlation between salinity and R. mangle $\delta^2 H_{taraxerol}$, $\delta^2 H_{lupeol}$ or $\delta^2 H_{n-C31~alkane}$ suggests that $\delta^2 H$ values of fatty acids have different responses to salinity than do n-alkanes or triterpenoids (Supplementary Fig. S4). Therefore, fractionation during biosynthesis of isoprenoids and longer-chain acetogenic lipids may be responsible for a significant portion of the negative correlations between salinity and α²H_{lipid-water} for these compounds in uncultivated mangroves.

4.2.2. Influence of $\delta^2 H_{lw}$ on $\delta^2 H_{fatty\ acid}$

The relationship between salinity and $\delta^2 H$ values of leaf water $(\delta^2 H_{lw})$ can partially account for enrichment of greenhouse-cultivated mangrove $\delta^2 H_{fatty\ acid}$ values with increasing salinity. Plant leaf water is a major source of hydrogen in lipids produced by dicots, and $\delta^2 H_{lw}$ values depend on variables including temperature, relative humidity, stomatal conductance, transpiration rate, $\delta^2 H_{water}$ and $\delta^2 H_{xw}$ (Schmidt et al., 2003; Kahmen et al., 2011a, 2013). Therefore, if any of these variables are correlated with salinity, $\delta^2 H_{lw}$ would also be expected to vary with salinity, and lipids produced from leaf water will have different $\delta^2 H$ values.

The effects on $\delta^2 H_{lw}$ of environmental parameters that vary with salinity (e.g., stomatal conductance, $\delta^2 H_{xw}$ and path length) were assessed with a Péclet-modified Craig-Gordon leaf water isotope model (Kahmen et al., 2011b). $\delta^2 H_{lw}$ values became enriched by 3‰ as stomatal conductance decreased across the range expected for salinity ranging between 5 and 30 ppt. However, $\delta^2 H_{lw}$ values at 30 ppt were $^2 H$ -depleted by 2.7‰ due to $\delta^2 H_{xw}$ decreasing by 7.6‰ across the 25 ppt salinity range. In addition, at 30 ppt salinity, leaf water was $^2 H$ -depleted by 3‰ relative to 5 ppt salinity, as path length increased from 120 mm to 280 mm. Therefore, $\delta^2 H_{lw}$ values were expected to be depleted by 2.7‰ at higher salinity, which is opposite to the observed $\delta^2 H_{fatty~acid}$ variability across salinities.

The combined effects of diurnally varying environmental parameters (e.g., air temperature, relative humidity and $\delta^2 H_{\text{atmospheric vapor}})$ were assessed with the same leaf water model. Because plants under high salt-stress display diurnal variations in WUE and photosynthetic activity (Naidoo and von Willert, 1995; Barr et al., 2009), and photosynthetic activity is related to fatty acid production (Delwiche and Sharkey, 1993; Bao et al., 2000), preferential sourcing of lipid-hydrogen from either an ²H-depleted daytime, or ²H-enriched nighttime leaf water pool could impact δ²H_{fatty acid} values. Different species of mangroves (A. germinans, A. annulata and R. mangle) growing under high salinity minimize evaporative water loss during midday, when both air temperature and vapor pressure deficit are highest, by maintaining high photosynthetic rates and low WUE in early morning (Naidoo and von Willert, 1995; Barr et al., 2009). Newly fixed carbon in plants is utilized for fatty acid or isoprene synthesis within 2-3 min (Delwiche and Sharkey, 1993; Bao et al., 2000). If fixed carbon is used for fatty

acid production very quickly after it is assimilated, fatty acid production is also likely to be more active when the plant is photosynthetically more active. Therefore, if the mangroves cultivated at high salinity in our study exhibited highest photosynthetic performance in the morning to avoid water loss, the lipids produced may have incorporated the δ^2 H composition of the nighttime leaf-water pool, which the leaf water model predicts would be enriched by 16% relative to the daytime leaf-water pool. Mangroves growing at low salinity, on the other hand, would be relatively less sensitive to water loss, and their lipids, by extension, less impacted by the ²H-enriched nighttime leaf-water pool, which would result in more ²H-depleted lipids. Integrated with the result above, while plants growing at high salinity draw from a leaf-water pool depleted by 3% relative to plants growing at low salinity, if their lipid synthesis relies more on the enriched nighttime leaf-water pool, this mechanism alone can account for about half of the entire 22-24% variability in $\delta^2 H_{fatty\ acid}$ of R. mangle and X. granatum, or about a quarter of the 48–64‰ variability in $\delta^2 H_{fatty\ acid}$ of R. apiculata.

Differences in $\delta^2 H_{fatty\ acid}$ values or trends with salinity among species may be due to species-specific physiological processes for salt management that result in different leaf water potential and leaf water enrichment. For example, effective salt secretion may influence the proportion of more or less enriched leaf water pool during day and night that gets incorporated into lipids. In our study, A. germinans and L. racemosa were the only species (of the five) that are known to secrete salt from their leaves, and $\delta^2 H_{fatty\ acid}$ values of both species were uncorrelated with salinity. High efficiency of salt secretion may be maintained by daily variations in transpiration rates to keep xylem water potential very low during the day (Waisel et al., 1986). Therefore, effective salt secretion may have helped A. germinans and L. racemosa in high salinity treatments to be less sensitive to water loss during midday and less reliant on the enriched nighttime leaf water pool relative to other species. Different biophysical processes of species relying on the same salt management strategies may also affect water potentials. For example, while A. germinans and Rhizophora spp. are both capable of accumulating salt in leaf vacuoles and producing organic solutes, different types and concentrations of compatible solutes produced by each species may also affect osmotic potentials to different degrees (Popp et al., 1985). In addition, distinct compatible solutes produced by different species may have a larger impact on $\delta^2 H_{lipid}$ values than on $\delta^2 H_{water}$ values, as types and varying proportions of compatible solutes in different salt marsh plants or mangrove species may result in varying contributions of hydrogen in alkanes and fatty acids from photosynthetic and metabolic NADPH pools (Ladd and Sachs, 2015a; Eley et al., 2018).

4.2.3. Potential reliance on stored carbohydrates

The different relationship between lipid δ^2 H values and salinity from greenhouse-cultivated and uncultivated mangroves may also be explained by greenhouse seedlings relying on stored carbohydrates in large propagules during fatty acid synthesis. Hydrogen in lipids is derived from leaf water and NADPH from either photosynthesis or sugar metabolism (Schmidt et al., 2003). When plants synthesize lipids from stored carbohydrates, hydrogen can come from NADPH either in the chloroplast (produced by photosynthesis) or in the cytosol (produced by sugar metabolism), and photosynthetic NADPH is expected to be depleted in ²H relative to metabolic NADPH by as much as several hundred per mil (Schmidt et al., 2003). If photosynthetic activity is limited during lipid synthesis, plants are more likely to rely on NADPH from the cytosol, producing more ²H-enriched lipids (Schmidt et al., 2003; Cormier et al., 2018). Several studies have observed ²H-enriched n-alkanes in leaf waxes of angiosperms that were photosynthetically limited and reliant on stored carbohydrates in large seeds (Newberry et al., 2015; Freimuth et al., 2017; Cormier et al., 2018).

Weights of mangrove seeds vary widely between species, but the two genera that showed significant correlation between salinity and $\delta^2 H_{lipid}$ in our study have very large seeds. X. granatum seeds typically weigh 45-77 g, while Rhizophora species propagules weigh 14-30 g (Rabinowitz, 1978; Smith, 1987; Gokhale and Chavan, 2002; Das and Ghose, 2003), and 40-60% of the propagule mass is in the form of starch and sugar, potentially providing a long-lasting carbohydrate source (Smith, 1987; Gunawan et al., 2013). If mangrove seedlings growing at high salinity had limited photosynthetic capability and relied more on stored carbohydrates in propagules for lipid production, contributions of H derived from the ²H-enriched metabolic NADPH pool would be larger than that from the ²H-depleted photosynthetic NADPH pool, so lipids would be more enriched in ²H (Newberry et al., 2015; Cormier et al., 2018). This trend is expected to be more pronounced in alkanes or isoprenoids than in fatty acids, which have relatively short turnover times (Sachse et al., 2009; Kahmen et al., 2011a; Gao et al., 2012). In our study, δ^2 H values of triterpenoids extracted from R. mangle leaves harvested in 2016 were more depleted than those extracted from leaves harvested in 2014 (Fig. 5), supporting the possibility that lipid-hydrogen was derived in part from carbohydrates stored in propagules and large seeds. As the plants matured they presumably relied less on those maternal reserves and more on their photosynthetic capacity.

In summary, the relationships between $\delta^2 H_{lipid}$ values and salinity were different for fatty acids produced by three cultivated mangrove species (R. apiculata, R. mangle and X. granatum) than for n-alkanes and triterpenols from seven mangrove species in diverse natural settings (Ladd and Sachs, 2012, 2015a, 2015b, 2017; He et al., 2017). In order to be able to improve uncertainties in the relationship between $\alpha^2 H$ and salinity using greenhouse-cultivated mangroves, a better understanding of the impact of salinity on $\alpha^2 H$ is necessary. For instance, if the difference is largely due to a lack of $^2 H$ -depleted freshwater sources in the greenhouse, improved calibrations might only be possible if alternate freshwater sources can be provided in the greenhouse.

4.3. Implications of $\delta^2 H$ and $\delta^{13} C_{fatty\ acid}$ measurements from greenhouse-cultivated mangroves for reconstructing precipitation rates

The use of coupled δ^2H and $\delta^{13}C$ values of mangrove lipids holds promise for quantitatively reconstructing precipitation rates in the past, a climate parameter for which there are few proxies at present. In order to do so, salinity and δ^2H_{water} values are calculated from the definition of α ($\alpha^2H=(\delta^2H_{lipid}+1000)/(\delta^2H_{water}+1000)$ and $\alpha^{13}C=(\delta^{13}C_{lipid}+1000)/(\delta^{13}C_{atm}+1000))$ and the linear relationships between α and salinity ($\alpha^2H=m_2\times S+b_2$ and $\alpha^{13}C=m_{13}\times S+b_{13})$, as implied in Eqs. (1) and (2). Representative slopes and intercepts were $m_2=-0.0015\pm0.000026,\ b_2=0.892\pm0.0057,\ m_{13}=0.00019\pm0.000053$ and $b_{13}=0.970\pm0.0012$ (calibrations from A. marina n-C_{31} alkanes; Ladd and Sachs, 2012, 2013). We assessed uncertainties in the derived salinity and δ^2H_{water} values using a 1000-iteration Monte Carlo simulation that included both calibration and analytical uncertainties for both δ^2H and $\delta^{13}C$.

$$\mbox{Salinity} = \left(\frac{\left(\delta^{13} \mbox{C_{lipid}} + 1000 \right)}{\left(\delta^{13} \mbox{C_{atm}} + 1000 \right)} - \ \mbox{b_{13}} \right) \times \frac{1}{m_{13}} \eqno(1)$$

$$\delta^2 H_{water} = \left(\frac{\left(\delta^2 H_{lipid} + 1000 \right)}{\frac{m_2}{m_{13}} \left(\frac{\left(\delta^{13} C_{lipid} + 1000 \right)}{\left(\delta^{13} C_{atm} + 1000 \right)} - b_{13} \right) + b_2} \right) - 1000 \tag{2}$$

To evaluate the effect that reducing uncertainties in the calibrations of both $\alpha^2 H$ and $\alpha^{13} C$ with salinity would have on the uncertainty of the derived salinity and $\delta^2 H_{water}$ values, several 1000-iteration Monte Carlo analyses with a surrogate data point were performed $(\delta^2 H_{lipid} = -100 \pm 5 \%, \ \delta^{13} C_{lipid} = -30 \pm 0.3 \%),$ assuming a 50% and 100% reduction in the calibration uncertainties and propagating the reduced errors to calculate uncertainties in salinity and $\delta^2 H_{water}$. Results of these analyses (Table 7) indicate that reducing uncertainty in the $\alpha^{13} C$ -salinity calibration alone can reduce as much uncertainties in both the $\alpha^2 H$ -salinity and $\alpha^{13} C$ -salinity calibrations. Future work should therefore focus on obtaining improved $\alpha^{13} C$ -salinity calibrations from both field and laboratory-based studies, possibly by increasing the number of samples to be analyzed.

Future work should also focus on measuring H and C isotopes of source-specific biomarkers. We have used slopes and intercepts from $n-C_{31}$ alkanes for the uncertainty analysis above to demonstrate how the paired H and C isotope approach would work, and focused on n-C₁₆ and n-C₁₈ fatty acid δ^2 H and δ^{13} C measurements to gain more insight into the mechanisms that control H and C isotope fractionation as a function of salinity in mangrove lipids. However, n- C_{16} , n- C_{18} fatty acids and n-alkanes are produced not only by mangroves, but also by terrestrial vascular plants, phytoplankton, and bacteria (e.g., Bianchi and Canuel, 2011). Therefore, it would be virtually impossible to discern whether fatty acids or n-alkanes in mangrove swamps and coastal sediments originated from mangroves or other organisms. Because hydrogen and carbon isotope fractionation in lipids produced by organisms other than mangroves may respond differently to salinity, application of paired $\delta^2 H$ and $\delta^{13} C$ of fatty acids or alkanes with unknown sources cannot provide reasonable estimates of salinity and $\delta^2 H_{water}$. A promising alternative to fatty acids and n-alkanes is taraxerol, which in mangroves is primarily produced by Rhizophora spp. (Versteegh et al., 2004; Koch et al., 2005), which are dominant in many tropical mangrove forests (Duke, 2006). Since taraxerol found in coastal tropical and subtropical sediments is likely to be derived from mangroves, applying the paired δ^2H and $\delta^{13}C$ approach with taraxerol is a promising approach for constructing past precipitation rates.

In addition, for future mangrove culturing studies that may be conducted to improve the calibrations between salinity and $\delta^2 H$ or $\delta^{13} C$ of mangrove-derived lipids, the culturing could simulate field conditions more closely. For instance, temperature and relative humidity inside the greenhouse could be set higher to better mimic tropical climate conditions and protect trees from possible cold stress. Also, transferring plants to larger pots more often would prevent possible inhibition of growth by root restriction.

5. Conclusions

 $\delta^{13}C$ and δ^2H values of $n\text{-}C_{16}$ and $n\text{-}C_{18}$ fatty acids and $\delta^{13}C$ values of bulk leaves in five species of mangroves cultivated in salinity treatments of 5–30 ppt in the UW greenhouse were measured. Both $\delta^{13}C_{\text{fatty acids}}$ and $\delta^{13}C_{\text{bulk leaf}}$ values from three species (*L. racemosa, R. apiculata,* and *X. granatum*) were positively correlated with salinity (0.12–0.21‰/ppt and 0.10–0.22‰/ppt, respectively), due to increased WUE and ^{13}C -enriched internal CO₂ pool with increasing salinity.

 $\delta^2 H_{fatty\ acids}$ values from three species ($R.\ apiculata,\ R.\ mangle,$ and $X.\ granatum$) were positively correlated with salinity (0.47–1. 25%/ppt), opposite to all field studies up to date, most likely due to lack of 2H -depleted freshwater in the greenhouse. The positive relationship observed between salinity and $\delta^2 H_{fatty\ acids}$ in greenhouse-cultivated mangroves may be caused by temporal

	Salinity (ppt)	Salinity error (ppt)	$\delta^2 H_{water} (\%)$	$\delta^2 H_{water}$ error (‰)
100% uncertainty in C & H	43.07	3.08	87.93	6.09
50% uncertainty in C & H	43.18	1.69	88.13	3.34
50% uncertainty in only H	43.16	3.26	88.11	6.47
50% uncertainty in only C	43.21	1.70	88.18	3.36
0% uncertainty in C & H	43.26	0.52	88.26	1.02

variation in $\delta^2 H_{leaf\ water}$ values and timing of lipid production, or reliance on stored carbohydrates in seeds.

To use paired $\delta^2 H$ and $\delta^{13} C$ measurements of mangrove lipids to quantitatively reconstruct salinity and water isotopes, $\delta^2 H$ and $\delta^{13} C$ values of mangrove-specific biomarkers such as taraxerol should be measured. In addition, improving field and laboratory-based calibrations between salinity and $\alpha^{13} C$, partly by cultivating mangroves under an environment that resembles tropical or subtropical climate more closely, will be important for future studies. At this point, improving field and laboratory-based calibrations between salinity and $\alpha^{13} C$ will be most likely to reduce uncertainties in estimated salinity and water isotopes.

Acknowledgements

This work was supported by the National Science Foundation under Grants No. EAR-1348396 and OCE-1736222 (J.P.S.). Erick Waguk assisted with seed collection in Micronesia. Doug Ewing, June Landenburger, Marta Wolfshorndl, Colton Skavicus, Cyrena Thibodeau, Josh Gregersen and Tory Johnson assisted with mangrove cultivation in the greenhouse. Matthew Wolhowe, Mark Haught, Ashley Maloney and Tess Clinkingbeard provided assistance and advice with isotope measurements and other analytical techniques. Paul Quay, Jodi Young, Steve Emerson and Liz van Volkenberg provided constructive feedback and comments that greatly improved both this study and this manuscript. Two anonymous reviewers provided helpful feedback and comments that improved this manuscript. We are grateful for all their contributions.

Appendix A. Supplementary material

Supplementary data to this article can be found online at https://doi.org/10.1016/j.orggeochem.2019.03.001.

Associate Editor-Kliti Grice

References

- Alongi, D.M., Mukhopadhyay, S.K., 2015. Contribution of mangroves to coastal carbon cycling in low latitude seas. Agricultural and Forest Meteorology 213, 266–272.
- Arnold, T.E., Diefendorf, A.F., Brenner, M., Freeman, K.H., Baczynski, A.A., 2018. Climate response of the Florida Peninsula to Heinrich events in the North Atlantic. Quaternary Science Reviews 194, 1–11.
- Arp, W.J., 1991. Effects of source-sink relations on photosynthetic acclimation to elevated CO₂. Plant, Cell and Environment 14, 869–875.
- Atwood, A.R., Sachs, J.P., 2014. Separating ITCZ- and ENSO-related rainfall changes in the Galápagos over the last 3 kyr using D/H ratios of multiple lipid biomarkers, Earth and Planetary Science Letters 404, 408–419.
- Ball, M.C., Farquhar, G.D., 1983. Photosynthetic and stomatal responses of two mangrove species, *Aegiceras corniculatum* and *Avicennia marina*, to long term salinity and humidity conditions. Plant Physiology 74, 1–6.
- Bao, X., Focke, M., Pollard, M., Ohlrogge, J., 2000. Understanding *in vivo* carbon precursor supply for fatty acid synthesis in leaf tissue. Plant Journal 22, 39–50.
 Barr, J.G., Fuentes, J.D., Engel, V., Zieman, J.C., 2009. Physiological responses of red mangroves to the climate in the Florida Everglades. Journal of Geophysical Research: Biogeosciences 114, 1–13.
- Bianchi, T.S., Canuel, E.A., 2011. Chemical Biomarkers in Aquatic Ecosystems. Princeton University Press, Princeton, New Jersey.

- Biber, P.D., 2006. Measuring the effects of salinity stress in the red mangrove, *Rhizophora mangle* L. African Journal of Agricultural Research 1, 1–4.
- Bony, S., Risi, C., Vimeux, F., 2008. Influence of convective processes on the isotopic composition (δ¹⁸O and δD) of precipitation and water vapor in the tropics: 1. Radiative-convective equilibrium and tropical ocean-global atmosphere-coupled ocean-atmosphere response experiment (TOGA-COARE) simulations. Journal of Geophysical Research Atmospheres 113, 1–21.
- Brugnoli, E., Lauteri, M., Istituto, C.N.R., 1991. Effects of salinity on stomatal conductance, photosynthetic capacity, and carbon isotope discrimination of salt-tolerant (*Gossypium hirsutum L.*) and salt-sensitive (*Phaseolus vulgaris L.*) C3 non-halophytes. Plant Physiology 95, 628–635.
- Cheng, H., Tam, N.F.Y., Wang, Y., Li, S., Chen, G., Ye, Z., 2012. Effects of copper on growth, radial oxygen loss and root permeability of seedlings of the mangroves *Bruguiera gymnorrhiza* and *Rhizophora stylosa*. Plant and Soil 359, 255–266.
- Chiang, J.C.H., 2009. The tropics in paleoclimate. Annual Review of Earth and Planetary Sciences 37, 263–297.
- Chivall, D., M'Boule, D., Sinke-Schoen, D., Sinninghe Damsté, J.S., Schouten, S., van der Meer, M.T.J., 2014. The effects of growth phase and salinity on the hydrogen isotopic composition of alkenones produced by coastal haptophyte algae. Geochimica et Cosmochimica Acta 140, 381–390.
- Cormier, M.A., Werner, R.A., Sauer, P.E., Gröcke, D.R., Leuenberger, M.C., Wieloch, T., Schleucher, J., Kahmen, A., 2018. ²H-fractionations during the biosynthesis of carbohydrates and lipids imprint a metabolic signal on the δ²H values of plant organic compounds. New Phytologist 218, 479–491.
- Dansgaard, W., 1964. Stable isotopes in precipitation. Tellus 16, 436-468.
- Das, S., Ghose, M., 2003. Seed structure and germination pattern of some Indian mangroves with taxonomic relevance. Taiwania 48, 287–298.
- Delwiche, C.F., Sharkey, T.D., 1993. Rapid appearance of ¹³C in biogenic isoprene when ¹³CO₂ is fed to intact leaves. Plant, Cell and Environment 16, 587–591.
- Douglas, P.M.J., Pagani, M., Brenner, M., Hodell, D.A., Curtis, J.H., 2012. Aridity and vegetation composition are important determinants of leaf-wax δD values in southeastern Mexico and Central America. Geochimica et Cosmochimica Acta 97, 24–45.
- Duke, N.C., 2006. Australia's Mangroves: The Authoritative Guide to Australia's Mangrove Plants. University of Queensland, Brisbane, Australia.
- Eley, Y., White, J., Dawson, L., Hren, M., Pedentchouk, N., 2018. Variation in hydrogen isotope composition among salt marsh plant organic compounds highlights biochemical mechanisms controlling biosynthetic fractionation. Journal of Geophysical Research: Biogeosciences 123, 2645–2660.
- Ellsworth, P.V., Ellsworth, P.Z., Anderson, W.T., Sternberg, L.S., 2013. The role of effective leaf mixing length in the relationship between the δ^{18} O of stem cellulose and source water across a salinity gradient. Plant, Cell and Environment 36, 138–148.
- Englebrecht, A.C., Sachs, J.P., 2005. Determination of sediment provenance at drift sites using hydrogen isotopes and unsaturation ratios in alkenones. Geochimica et Cosmochimica Acta 69, 4253–4265.
- Ewe, S.M.L., Sternberg, L.D.S.L., Childers, D.L., 2007. Seasonal plant water uptake patterns in the saline southeast Everglades ecotone. Oecologia 152, 607–616.
- Fairbanks, R.G., Evans, M.N., Rubenstone, J.L., Mortlock, R.A., Broad, K., Moore, M.D., Charles, C.D., 1997. Evaluating climate indices and their geochemical proxies measured in corals. Coral Reefs 16, S93–S100.
- Farquhar, G., O'Leary, M., Berry, J., 1982. On the relationship between carbon isotope discrimination and the intercellular carbon dioxide concentration in leaves. Australian Journal of Plant Physiology 9, 121–137.
- Farquhar, G.D., Ehlerginer, J.R., Hubick, K.T., 1989. Carbon isotope discrimination and photosynthesis. Annual Review of Plant Physiology 40, 503–537.
- Feakins, S.J., Sessions, A.L., 2010. Controls on the D/H ratios of plant leaf waxes in an arid ecosystem. Geochimica et Cosmochimica Acta 74, 2128–2141.
- Flato, G., Marotzke, J., Abiodun, B., Braconnot, P., Chou, S.C., Collins, W., Cox, P., Driouech, F., Emori, S., Eyring, V., Forest, C., Gleckler, P., Guilyardi, E., Jakob, C., Kattsov, V., Reason, C., Rummukainen, M., 2013. Evaluation of climate models. In: Stocker, T.F., Qin, D., Plattner, G.-K., Tignor, M., Allen, S.K., Boschung, J., Nauels, A., Xia, Y., Bex, V., Midgley, P.M. (Eds.), Climate Change 2013: The Physical Science Basis. Contribution of Working Group I to the Fifth Assessment Report of the Intergovernmental Panel on Climate Change. Cambridge University Press, Cambridge, UK and New York. USA.
- Freimuth, E.J., Diefendorf, A.F., Lowell, T.V., 2017. Hydrogen isotopes of *n*-alkanes and *n*-alkanoic acids as tracers of precipitation in a temperate forest and implications for paleorecords. Geochimica et Cosmochimica Acta 206, 166–183.
- Gao, L., Burnier, A., Huang, Y., 2012. Quantifying instantaneous regeneration rates of plant leaf waxes using stable hydrogen isotope labeling. Rapid Communications in Mass Spectrometry 26, 115–122.

- Giri, C., Ochieng, E., Tieszen, L.L., Zhu, Z., Singh, A., Loveland, T., Masek, J., Duke, N., 2011. Status and distribution of mangrove forests of the world using earth observation satellite data. Global Ecology and Biogeography 20, 154–159.
- Gokhale, M.V., Chavan, N.S., 2002. Germination and growth performance of Xylocarpus granatum. In: Proceedings of the National Seminar on Creeks, Estuaries and Mangroves – Pollution and Conservation, November 2002, pp. 237–239.
- Greer, L., Swart, P.K., 2006. Decadal cyclicity of regional mid-Holocene precipitation: Evidence from Dominican coral proxies. Paleoceanography 21, 1–17
- Guenther, F., Aichner, B., Siegwolf, R., Xu, B., Yao, T., Gleixner, G., 2013. A synthesis of hydrogen isotope variability and its hydrological significance at the Qinghai-Tibetan Plateau. Quaternary International 313–314, 3–16.
- Gunawan, S., Darmawan, R., Nanda, M., Setiawan, A.D., Fansuri, H., 2013. Proximate composition of *Xylocarpus moluccensis* seeds and their oils. Industrial Crops and Products 41, 107–112.
- Guy, R.D., Warne, P.G., Reid, D.M., 1988. Stable carbon isotope ratio as an index of water-use efficiency in C3 halophytes – possible relationship to strategies for osmotic adjustment. In: Rundel, P.W., Ehleringer, J.R., Nagy, K.A. (Eds.), Stable Isotopes in Ecological Research. Ecological Studies (Analysis and Synthesis). Springer, New York.
- He, D., Ladd, S.N., Sachs, J.P., Jaffé, R., 2017. Inverse relationship between salinity and ²H/¹H fractionation in leaf wax *n*-alkanes from Florida mangroves. Organic Geochemistry 110. 1–12.
- Heinzelmann, S.M., Chivall, D., M'Boule, D., Sinke-Schoen, D., Villanueva, L., Sinninghe Damsté, J.S., Schouten, S., Van der Meer, M.T.J., 2015a. Comparison of the effect of salinity on the D/H ratio of fatty acids of heterotrophic and photoautotrophic microorganisms. FEMS Microbiology Letters 362, 1–6.
- Heinzelmann, S.M., Villanueva, L., Sinke-Schoen, D., Sinninghe Damsté, J.S., Schouten, S., van der Meer, M.T.J., 2015b. Impact of metabolism and growth phase on the hydrogen isotopic composition of microbial fatty acids. Frontiers in Microbiology 6, 1–11.
- Huang, Y., Shuman, B., Wang, Y., Webb, T., 2004. Hydrogen isotope ratios of individual lipids in lake sediments as novel tracers of climatic and environmental change: A surface sediment test. Journal of Paleolimnology 31, 363-375
- Jennerjahn, T.C., Ittekkot, V., 2002. Relevance of mangroves for the production and deposition of organic matter along tropical continental margins. Naturwissenschaften 89, 23–30.
- Jiang, Q., Roche, D., Monaco, T.A., Durham, S., 2006. Gas exchange, chlorophyll fluorescence parameters and carbon isotope discrimination of 14 barley genetic lines in response to salinity. Field Crops Research 96, 269–278.
- Jones, P.D., Briffa, K.R., Osborn, T.J., Lough, J.M., Van Ommen, T.D., Vinther, B.M., Luterbacher, J., Wahl, E.R., Zwiers, F.W., Mann, M.E., Schmidt, G.A., Ammann, C. M., Buckley, B.M., Cobb, K.M., Esper, J., Goosse, H., Graham, N., Jansen, E., Kiefer, T., Kull, C., Küttel, M., Mosley-Thompson, E., Overpeck, J.T., Riedwyl, N., Schulz, M., Tudhope, A.W., Villalba, R., Wanner, H., Wolff, E., Xoplaki, E., 2009. Highresolution paleoclimatology of the last millennium: A review of current status and future prospects. Holocene 19, 3–49.
- Kahmen, A., Dawson, T.E., Vieth, A., Sachse, D., 2011a. Leaf wax n-alkane δD values are determined early in the ontogeny of Populus trichocarpa leaves when grown under controlled environmental conditions. Plant, Cell and Environment 34, 1639–1651.
- Kahmen, A., Sachse, D., Arndt, S.K., Tu, K.P., Farrington, H., Vitousek, P.M., Dawson, T. E., 2011b. Cellulose δ^{18} O is an index of leaf-to-air vapor pressure difference (VPD) in tropical plants. Proceedings of the National Academy of Sciences 108, 1981–1986.
- Kahmen, A., Hoffmann, B., Schefuß, E., Arndt, S.K., Cernusak, L.A., West, J.B., Sachse, D., 2013. Leaf water deuterium enrichment shapes leaf wax *n*-alkane δD values of angiosperm plants II: Observational evidence and global implications. Geochimica et Cosmochimica Acta 111, 50–63.
- Kasai, M., Koide, K., Ichikawa, Y., 2012. Effect of pot size on various characteristics related to photosynthetic matter production in soybean plants. International Journal of Agronomy 2012, 1–7.
- Koch, B.P., Harder, J., Lara, R.J., Kattner, G., 2005. The effect of selective microbial degradation on the composition of mangrove derived pentacyclic triterpenols in surface sediments. Organic Geochemistry 36, 273–285.
- Konecky, B.L., Russell, J.M., Rodysill, J.R., Vuille, M., Bijaksana, S., Huang, Y., 2013. Intensification of southwestern Indonesian rainfall over the past millennium. Geophysical Research Letters 40, 386–391.
- Krauss, K.W., Allen, J.A., 2003. Influences of salinity and shade on seedling photosynthesis and growth of two mangrove species, *Rhizophora mangle* and *Bruguiera sexangula*, introduced to Hawaii. Aquatic Botany 77, 311– 224.
- Ladd, S.N., Sachs, J.P., 2012. Inverse relationship between salinity and n-alkane δD values in the mangrove *Avicennia marina*. Organic Geochemistry 48, 25–36.
- Ladd, S.N., Sachs, J.P., 2013. Positive correlation between salinity and n-alkane δ^{13} C values in the mangrove *Avicennia marina*. Organic Geochemistry 64, 1–8.
- Ladd, S.N., Sachs, J.P., 2015a. Hydrogen isotope response to changing salinity and rainfall in Australian mangroves. Plant, Cell and Environment 38, 2674–2687.
- Ladd, S.N., Sachs, J.P., 2015b. Influence of salinity on hydrogen isotope fractionation in *Rhizophora* mangroves from Micronesia. Geochimica et Cosmochimica Acta 168, 206–221.
- Ladd, S.N., Sachs, J.P., 2017. ²H/¹H fractionation in lipids of the mangrove *Bruguiera gymnorhiza* increases with salinity in marine lakes of Palau. Geochimica et Cosmochimica Acta 204, 300–312.

- Ladd, S.N., Nelson, D.B., Schubert, C.J., Dubois, N., 2018. Lipid compound classes display diverging hydrogen isotope responses in lakes along a nutrient gradient. Geochimica et Cosmochimica Acta 237, 103–119.
- Lambs, L., Muller, E., Fromard, F., 2008. Determination of ¹³C/¹²C ratios of endogenous urinary steroids: method validation, reference population and application to doping control purposes. Rapid Communications in Mass Spectrometry 22, 2161–2175.
- Li, Z.H., Labbé, N., Driese, S.G., Grissino-Mayer, H.D., 2011. Micro-scale analysis of tree-ring δ¹⁸O and δ¹³C on α-cellulose spline reveals high-resolution intraannual climate variability and tropical cyclone activity. Chemical Geology 284, 138–147.
- Liang, J., Wright, J.S., Cui, X., Sternberg, L., Gan, W., Lin, G., 2018. Leaf anatomical traits determine the ¹⁸O enrichment of leaf water in coastal halophytes. Plant, Cell and Environment 41, 2744–2757.
- Lin, G.H., Sternberg, L., 1992. Effect of growth form, salinity, nutrient and sulfide on photosynthesis, carbon isotope discrimination and growth of red mangrove (*Rhizophora mangle L.*). Functional Plant Biology 19, 509–517.
- Lin, G., Sternberg, L., 1993. Hydrogen isotopic fractionation by plant roots during water uptake in coastal wetland plants. In: Ehleringer, J.R., Hall, A.E., Farquhar, G.D. (Eds.), Stable Isotopes and Plant Carbon-Water Relations. Academic Press, San Diego, pp. 497–510.
- Lovelock, C.E., Reef, R., Ball, M.C., 2017. Isotopic signatures of stem water reveal differences in water sources accessed by mangrove tree species. Hydrobiologia 803. 133–145.
- M'boule, D., Chivall, D., Sinke-Schoen, D., Sinninghe Damsté, J.S., Schouten, S., Van der Meer, M.T.J., 2014. Salinity dependent hydrogen isotope fractionation in alkenones produced by coastal and open ocean haptophyte algae. Geochimica et Cosmochimica Acta 130, 126–135.
- Maloney, A.E., Shinneman, A.L.C., Hemeon, K., Sachs, J.P., 2016. Exploring lipid ²H/¹H fractionation mechanisms in response to salinity with continuous cultures of the diatom *Thalassiosira pseudonana*. Organic Geochemistry 101, 154–165.
- Maloney, A.E., Nelson, D.B., Richey, J.N., Prebble, M., Sear, D.A., Hassall, J.D., Langdon, P.G., Croudace, I.W., Zawadzki, A., Sachs, J.P., 2019. Reconstructing precipitation in the tropical South Pacific from dinosterol ²H/¹H ratios in lake sediment. Geochimica et Cosmochimica Acta 245, 190–206.
- Martin, K.C., Bruhn, D., Lovelock, C.E., Feller, I.C., Evans, J.R., Ball, M.C., 2010. Nitrogen fertilization enhances water-use efficiency in a saline environment. Plant, Cell and Environment 33, 344–357.
- Naidoo, G., von Willert, D.J., 1995. Diurnal gas exchange characteristics and water use efficiency of three salt-secreting mangroves at low and high salinities. Hydrobiologia 295, 13–22.
- Nelson, D.B., Sachs, J.P., 2014. The influence of salinity on D/H fractionation in dinosterol and brassicasterol from globally distributed saline and hypersaline lakes, Geochimica et Cosmochimica Acta 133, 325–339.
- Nelson, D.B., Sachs, J.P., 2016. Galápagos hydroclimate of the Common Era from paired microalgal and mangrove biomarker ²H/¹H values. Proceedings of the National Academy of Sciences 113, 3476–3481.
- NeSmith, D.S., Duval, J.R., 1998. The effect of container size. HortTechnology 8, 495–498.
- Newberry, S.L., Kahmen, A., Dennis, P., Grant, A., 2015. *n*-alkane biosynthetic hydrogen isotope fractionation is not constant throughout the growing season in the riparian tree *Salix viminalis*. Geochimica et Cosmochimica Acta 165, 75–85.
- Niedermeyer, E.M., Schefuß, E., Sessions, A.L., Mulitza, S., Mollenhauer, G., Schulz, M., Wefer, G., 2010. Orbital- and millennial-scale changes in the hydrologic cycle and vegetation in the western African Sahel: Insights from individual plant wax δD and δ¹³C. Quaternary Science Reviews 29, 2996–3005.
- Pahnke, K., Sachs, J.P., Keigwin, L., Timmermann, A., Xie, S.P., 2007. Eastern tropical Pacific hydrologic changes during the past 27,000 years from D/H ratios in alkenones. Paleoceanography 22, 1–15.
- Parida, A.K., Jha, B., 2010. Salt tolerance mechanisms in mangroves: a review. Trees 24, 199–217.
- Pfeiffer, M., Timm, O., Dullo, W.C., Garbe-Schönberg, D., 2006. Paired coral Sr/Ca and δ¹⁸O records from the Chagos Archipelago: Late twentieth century warming affects rainfall variability in the tropical Indian Ocean. Geology 34, 1069–1072.
- Pierrehumbert, R.T., 2000. Climate change and the tropical Pacific: The sleeping dragon wakes. Proceedings of the National Academy of Sciences 97, 1355–1358.
- Polissar, P.J., Freeman, K.H., 2010. Effects of aridity and vegetation on plant-wax δD in modern lake sediments. Geochimica et Cosmochimica Acta 74, 5785–5797.
- Poorter, H., Bühler, J., Van Dusschoten, D., Climent, J., Postma, J.A., 2012. Pot size matters: A meta-analysis of the effects of rooting volume on plant growth. Functional Plant Biology 39, 839–850.
- Popp, M., Larher, F., Weigel, P., 1985. Osmotic adaption in Australian mangroves. In: Ecology of Coastal Vegetation. Springer, Dordrecht, pp. 247–253.
- Rabinowitz, D., 1978. Mortality and initial propagule size in mangrove seedlings in Panama. Journal of Ecology 66, 45–51.
- Reef, R., Lovelock, C.E., 2015. Regulation of water balance in mangroves. Annals of Botany 115, 385–395.
- Richey, J.N., Sachs, J.P., 2016. Precipitation changes in the western tropical Pacific over the past millennium. Geology 44, 671–674.
- Risi, C., Bony, S., Vimeux, F., 2008. Influence of convective processes on the isotopic composition (8¹⁸O and 8D) of precipitation and water vapor in the tropics: 2. Physical interpretation of the amount effect. Journal of Geophysical Research Atmospheres 113. 1–12.
- Rivelli, A.R., James, R.A., Munns, R., Condon, A.G., 2002. Effect of salinity on water relations and growth of wheat genotypes with contrasting sodium uptake. Functional Plant Biology 29, 1065–1074.

- Sachs, J.P., Sachse, D., Smittenberg, R.H., Zhang, Z., Battisti, D.S., Golubic, S., 2009. Southward movement of the Pacific intertropical convergence zone AD 1400–1850. Nature Geoscience 2, 519–525.
- Sachs, J.P., Schwab, V.F., 2011. Hydrogen isotopes in dinosterol from the Chesapeake Bay estuary. Geochimica et Cosmochimica Acta 75, 444–459.
- Sachs, J.P., Kawka, O.E., 2015. The influence of growth rate on ²H/¹H fractionation in continuous cultures of the coccolithophorid *Emiliania huxleyi* and the diatom *Thalassiosira pseudonana*. PLoS One 10, 1–27.
- Sachs, J.P., Maloney, A.E., Gregersen, J., Paschall, C., 2016. Effect of salinity on ²H/¹H fractionation in lipids from continuous cultures of the coccolithophorid *Emiliania huxleyi*. Geochimica et Cosmochimica Acta 189, 96–109.
- Sachs, J.P., Maloney, A.E., Gregersen, J., 2017. Effect of light on ²H/¹H fractionation in lipids from continuous cultures of the diatom *Thalassiosira pseudonana*. Geochimica et Cosmochimica Acta 209, 204–215.
- Sachs, J.P., Stein, R., Maloney, A.E., Wolhowe, M., Fahl, K., Nam, S.I., 2018. An Arctic Ocean paleosalinity proxy from 8²H of palmitic acid provides evidence for deglacial Mackenzie River flood events. Quaternary Science Reviews 198, 76–90
- Sachse, D., Sachs, J.P., 2008. Inverse relationship between D/H fractionation in cyanobacterial lipids and salinity in Christmas Island saline ponds. Geochimica et Cosmochimica Acta 72, 793–806.
- Sachse, D., Kahmen, A., Gleixner, G., 2009. Significant seasonal variation in the hydrogen isotopic composition of leaf-wax lipids for two deciduous tree ecosystems (*Fagus sylvativa* and *Acerpseudoplatanus*). Organic Geochemistry 40, 732–742
- Sachse, D., Radke, J., Gleixner, G., 2004. Hydrogen isotope ratios of recent lacustrine sedimentary *n*-alkanes record modern climate variability. Geochimica et Cosmochimica Acta 68, 4877–4889.
- Sachse, D., Billault, I., Bowen, G.J., Chikaraishi, Y., Dawson, T.E., Feakins, S.J., Freeman, K.H., Magill, C.R., McInerney, F.A., van der Meer, M.T.J., Polissar, P., Robins, R.J., Sachs, J.P., Schmidt, H.-L., Sessions, A.L., White, J.W.C., West, J.B., Kahmen, A., 2012. Molecular Paleohydrology: Interpreting the hydrogenisotopic composition of lipid biomarkers from photosynthesizing organisms. Annual Review of Earth and Planetary Sciences 40, 221–249.
- Santini, N.S., Reef, R., Lockington, D.A., Lovelock, C.E., 2015. The use of fresh and saline water sources by the mangrove *Avicennia marina*. Hydrobiologia 745, 59–68.
- Sauer, P.E., Eglinton, T.I., Hayes, J.M., Schimmelmann, A., Sessions, A.L., 2001. Compound-specific D/H ratios of lipid biomarkers from sediments as a proxy for environmental and climatic conditions. Geochimica et Cosmochimica Acta 65, 213–222.
- Schefuß, E., Schouten, S., Schneider, R.R., 2005. Climatic controls on central African hydrology during the past 20,000 years. Nature 437, 1003–1006.
- Schmidt, H.L., Werner, R.A., Eisenreich, W., 2003. Systematics of ²H patterns in natural compounds and its importance for the elucidation of biosynthetic pathways. Phytochemistry Reviews 2, 61–85.
- Schouten, S., Ossebaar, J., Schreiber, K., Kienhuis, M.V.M., Langer, G., Benthien, A., Bijma, J., 2006. The effect of temperature, salinity and growth rate on the stable hydrogen isotopic composition of long chain alkenones produced by *Emiliania huxleyi* and *Gephyrocapsa oceanica*. Biogeosciences 3, 113–119.
- Smith III, T.J., 1987. Seed predation in relation to tree dominance and distribution in mangrove forests. Ecology 68, 266–273.
- Smith, F.A., Freeman, K.H., 2006. Influence of physiology and climate on δD of leaf wax *n*-alkanes from C3 and C4 grasses. Geochimica et Cosmochimica Acta 70, 1172–1187.
- Smittenberg, R.H., Saenger, C., Dawson, M.N., Sachs, J.P., 2011. Compound-specific D/H ratios of the marine lakes of Palau as proxies for West Pacific Warm Pool hydrologic variability. Quaternary Science Reviews 30, 921–933.
- Sobrado, M.A., 2000a. Leaf photosynthesis of the mangrove *Avicennia germinans* as affected by NaCl. Photosynthetica 36, 547–555.
- Sobrado, M.A., 2000b. Relation of water transport to leaf gas exchange properties in three mangrove species. Trees 14, 258–262.
- Song, X., Barbour, M.M., Farquhar, G.D., Vann, D.R., Helliker, B.R., 2013. Transpiration rate relates to within-and across-species variations in effective path length in a leaf water model of oxygen isotope enrichment. Plant, Cell and Environment 36, 1338–1351.
- Steppe, K., Vandegehuchte, M.W., Van de Wal, B.A.E., Hoste, P., Guyot, A., Lovelock, C.E., Lockington, D.A., 2018. Direct uptake of canopy rainwater causes turgor-

- driven growth spurts in the mangrove Avicennia marina. Tree Physiology 38, 979-991.
- Sternberg, L.D.S.L., Swart, P.K., 1987. Utilization of freshwater and ocean water by coastal plants of southern Florida. Ecology 68, 1898–1905.
- Sun, Q., Miao, C., Duan, Q., Ashouri, H., Sorooshian, S., Hsu, K.L., 2017. A review of global precipitation datasets: data sources, estimation, and intercomparisons. Reviews of Geophysics 56, 79–107.
- Thompson, L.G., Mosley-Thompson, E., Bolzan, J.F., Koci, B.R., 1985. A 1500-year record of tropical precipitation in ice cores from the Quelccaya Ice Cap, Peru. Science 229, 971–973.
- Thompson, L.G., Mosley-Thompson, E., Davis, M.E., Zagorodnov, V.S., Howat, I.M., Mikhalenko, V.N., Lin, P.N., 2013. Annually resolved ice core records of tropical climate variability over the past ∼1800 years. Science 340, 945–950.
- Tierney, J.E., Russell, J.M., Huang, Y., Sinninghe Damsté, J.S., Hopmans, E.C., Cohen, A. S., 2008. Northern hemisphere controls on tropical southeast African climate during the past 60,000 years. Science 322, 252–255.
- Tipple, B.J., Berke, M.A., Doman, C.E., Khachaturyan, S., Ehleringer, J.R., 2013. Leaf-wax *n*-alkanes record the plant-water environment at leaf flush. Proceedings of the National Academy of Sciences 110, 2659–2664.
- Tipple, B.J., Pagani, M., 2013. Environmental control on eastern broadleaf forest species' leaf wax distributions and D/H ratios. Geochimica et Cosmochimica Acta 111, 64–77.
- Tiwari, M., Ramesh, R., Somayajulu, B.L.K., Jull, A.J.T., Burr, G.S., 2006. Paleomonsoon precipitation deduced from a sediment core from the equatorial Indian Ocean. Geo-Marine Letters 26, 23–30.
- van der Meer, M.T.J., Benthien, A., French, K.L., Epping, E., Zondervan, I., Reichart, G. J., Bijma, J., Sinninghe Damsté, J.S., Schouten, S., 2015. Large effect of irradiance on hydrogen isotope fractionation of alkenones in *Emiliania huxleyi*. Geochimica et Cosmochimica Acta 160, 16–24.
- Versteegh, G.J.M., Schefuß, E., Dupont, L., Marret, F., Sinninghe Damsté, J.S., Jansen, J. H.F., 2004. Taraxerol and *Rhizophora* pollen as proxies for tracking past mangrove ecosystems. Geochimica et Cosmochimica Acta 68, 411–422.
- Vovides, A.G., Vogt, J., Kollert, A., Berger, U., Grueters, U., Peters, R., Lara-Domínguez, A.L., López-Portillo, J., 2014. Morphological plasticity in mangrove trees: salinity-related changes in the allometry of *Avicennia germinans*. Trees 28, 1413–1425.
- Waisel, Y., Eshel, A., Agami, M., 1986. Salt balance of leaves of the mangrove Avicennia marina. Physiologia Plantarum 67, 67–72.
- Wei, L., Lockington, D.A., Poh, S.C., Gasparon, M., Lovelock, C.E., 2013. Water use patterns of estuarine vegetation in a tidal creek system. Oecologia 172, 485–494.
- Weldeab, S., Lea, D.W., Schneider, R.R., Andersen, N., 2007. 155,000 years of West African monsoon and ocean thermal evolution. Science 316, 1303–1307.
- Wohl, E., Barros, A., Brunsell, N., Chappell, N.A., Coe, M., Giambelluca, T., Goldsmith, S., Harmon, R., Hendrickx, J.M.H., Juvik, J., McDonnell, J., Ogden, F., 2012. The hydrology of the humid tropics. Nature Climate Change 2, 655–662.
- Wolhowe, M.D., Prahl, F.G., Probert, I., Maldonado, M., 2009. Growth phase dependent hydrogen isotopic fractionation in alkenone-producing haptophytes. Biogeosciences 6, 1681–1694.
- Yang, H., Pagani, M., Briggs, D.E.G., Equiza, M.A., Jagels, R., Leng, Q., Lepage, B.A., 2009. Carbon and hydrogen isotope fractionation under continuous light: implications for paleoenvironmental interpretations of the High Arctic during Paleogene warming. Oecologia 160, 461–470.
- Zhang, Z., Sachs, J.P., 2007. Hydrogen isotope fractionation in freshwater algae: I. Variations among lipids and species. Organic Geochemistry 38, 582–608.
- Zhang, X., Zwiers, F.W., Hegerl, G.C., Lambert, F.H., Gillett, N.P., Solomon, S., Stott, P. A., Nozawa, T., 2007. Detection of human influence on twentieth-century precipitation trends. Nature 448, 461–465.
- Zhang, Z., Sachs, J.P., Marchetti, A., 2009. Hydrogen isotope fractionation in freshwater and marine algae: II. Temperature and nitrogen limited growth rate effects. Organic Geochemistry 40, 428–439.
- Zhang, Z., Leduc, G., Sachs, J.P., 2014. El Niño evolution during the Holocene revealed by a biomarker rain gauge in the Galápagos Islands. Earth and Planetary Science Letters 404, 420–434.
- Zhou, Y., Grice, K., Chikaraishi, Y., Stuart-Williams, H., Farquhar, G.D., Ohkouchi, N., 2011. Temperature effect on leaf water deuterium enrichment and isotopic fractionation during leaf lipid biosynthesis: results from controlled growth of C₃ and C₄ land plants. Phytochemistry 72, 207–213.